



**NAVAL
POSTGRADUATE
SCHOOL**

MONTEREY, CALIFORNIA

THESIS

**METEOROLOGICAL FACTORS THAT LEAD TO
SEPARATION OF THE CALIFORNIA COASTAL JET
FROM THE CENTRAL COAST**

by

Jonathan D. Mason

March 2007

Thesis Advisor:

Wendell A. Nuss

Second Reader:

Qing Wang

Approved for public release; distribution is unlimited.

THIS PAGE INTENTIONALLY LEFT BLANK

REPORT DOCUMENTATION PAGE		Form Approved OMB No. 0704-0188	
Public reporting burden for this collection of information is estimated to average 1 hour per response, including the time for reviewing instruction, searching existing data sources, gathering and maintaining the data needed, and completing and reviewing the collection of information. Send comments regarding this burden estimate or any other aspect of this collection of information, including suggestions for reducing this burden, to Washington headquarters Services, Directorate for Information Operations and Reports, 1215 Jefferson Davis Highway, Suite 1204, Arlington, VA 22202-4302, and to the Office of Management and Budget, Paperwork Reduction Project (0704-0188) Washington DC 20503.			
1. AGENCY USE ONLY (Leave blank)	2. REPORT DATE March 2007	3. REPORT TYPE AND DATES COVERED Master's Thesis	
4. TITLE AND SUBTITLE Meteorological Factors that Lead to Separation of the California Coastal Jet from the Central Coast		5. FUNDING NUMBERS	
6. AUTHOR(S) Jonathan D. Mason		8. PERFORMING ORGANIZATION REPORT NUMBER	
7. PERFORMING ORGANIZATION NAME(S) AND ADDRESS(ES) Naval Postgraduate School Monterey, CA 93943-5000		10. SPONSORING/MONITORING AGENCY REPORT NUMBER	
9. SPONSORING /MONITORING AGENCY NAME(S) AND ADDRESS(ES) N/A		11. SUPPLEMENTARY NOTES The views expressed in this thesis are those of the author and do not reflect the official policy or position of the Department of Defense or the U.S. Government.	
12a. DISTRIBUTION / AVAILABILITY STATEMENT Approved for public release; distribution is unlimited		12b. DISTRIBUTION CODE	
13. ABSTRACT (maximum 200 words) This study investigates the impact of off-shore cross-coast winds on the coastal-jet along the Central California Coast specifically Vandenberg AFB. Events that resulted in synoptic-scale offshore flow over most of the Central Californian coast were identified and considered for this study throughout the late spring through early fall 2006 season. A total of 18 events were found along the central coast during this time frame. Two case were selected from the 18 events for detailed analyses by examining the cross-coast offshore winds, length of duration, the degree of marine boundary layer compression, and westward migration of coastal jet. Results indicate changes in the California Coastal Jet are dominantly influenced by two major processes: subsidence due to increase of low to mid-level thickness above the boundary layer and downsloping winds directly above the marine boundary layer from flow over Coastal Mountain Ranges. Both processes lead to compression of the marine boundary layer near coast, increasing the east-west thermal gradient in the inversion above the marine boundary layer causing the coastal jet to migrate westward near the tightest temperature and pressure gradient.			
14. SUBJECT TERMS California Coastal Jet, marine boundary layer compression, offshore flow, Vandenberg AFB, subsidence, downsloping winds,		15. NUMBER OF PAGES 89	
		16. PRICE CODE	
17. SECURITY CLASSIFICATION OF REPORT Unclassified	18. SECURITY CLASSIFICATION OF THIS PAGE Unclassified	19. SECURITY CLASSIFICATION OF ABSTRACT Unclassified	20. LIMITATION OF ABSTRACT UL

NSN 7540-01-280-5500

Standard Form 298 (Rev. 2-89)
Prescribed by ANSI Std. 239-8

THIS PAGE INTENTIONALLY LEFT BLANK

Approved for public release; distribution is unlimited.

**METEOROLOGICAL FACTORS THAT LEAD TO SEPARATION OF THE
CALIFORNIA COASTAL JET FROM THE CENTRAL COAST**

Jonathan D. Mason
Captain, United States Air Force
B.S., University of Northern Colorado, 1998

Submitted in partial fulfillment of the
requirements for the degree of

MASTER OF SCIENCE IN METEOROLOGY

from the

**NAVAL POSTGRADUATE SCHOOL
March 2007**

Author: Jonathan D. Mason

Approved by: Wendell A. Nuss
Thesis Advisor

Qing Wang
Second Reader

Philip A. Durkee
Chairman, Department of Meteorology

THIS PAGE INTENTIONALLY LEFT BLANK

ABSTRACT

This study investigates the impact of off-shore cross-coast winds on the coastal-jet along the Central California Coast specifically Vandenberg AFB. Events that resulted in synoptic-scale offshore flow over most of the Central Californian coast were identified and considered for this study throughout the late spring through early fall 2006 season. A total of 18 events were found along the central coast during this time frame. Two cases were selected from the 18 events for detailed analyses by examining the cross-coast offshore winds, length of duration, the degree of marine boundary layer compression, and westward migration of coastal jet.

Results indicate changes in the California Coastal Jet are dominantly influenced by two major processes: subsidence due to increase of low to mid-level thickness above the boundary layer and downsloping winds directly above the marine boundary layer from flow over Coastal Mountain Ranges. Both processes lead to compression of the marine boundary layer near coast, increasing the east-west thermal gradient in the inversion above the marine boundary layer causing the coastal jet to migrate westward near the tightest temperature and pressure gradient.

THIS PAGE INTENTIONALLY LEFT BLANK

TABLE OF CONTENTS

I.	INTRODUCTION	1
A.	MOTIVATION	1
B.	VANDENBERG AFB GEOGRAPHY AND SUMMER CLIMATOLOGY	3
C.	PROBLEM STATEMENT	5
II.	BACKGROUND	7
A.	THE CALIFORNIA COASTAL JET	7
B.	VARIATIONS IN THE CALIFORNIA COASTAL JET	12
1.	Variations in Intensity	12
2.	Variations in Location	13
C.	POSSIBLE CAUSES OF COASTAL JET VARIATIONS	15
1.	Synoptic-scale Features	15
2.	Downsloping Wind Compression of the Boundary Layer	17
III.	DATA ANALYSIS	19
A.	DATA	19
1.	Atmospheric Model	19
2.	National Data Buoy Center Buoy Observations ..	22
IV.	RESULTS	25
A.	JUNE 20-24, 2006	25
1.	Synoptic Overview	25
2.	Coastal Jet Migration	31
3.	Marine Boundary Layer Changes	38
4.	June 20-24 Summary	42
B.	JULY 16-24, 2006	45
1.	Synoptic Overview	46
2.	Coastal Jet Migration	52
3.	Marine Boundary Layer Changes	56
4.	July 16-23 Summary	61
V.	CONCLUSIONS/RECOMMENDATIONS	63
A.	CONCLUSIONS	63
B.	RECOMMENDATIONS	66
	LIST OF REFERENCES	69
	INITIAL DISTRIBUTION LIST	71

THIS PAGE INTENTIONALLY LEFT BLANK

LIST OF FIGURES

Figure 1.	Map of Vandenberg AFB split into North and South region with wind tower sites denoted by number. (From 30 Weather Squadron Forecast Reference Notebook).....	2
Figure 2.	One of 26 Weather Towers located on Vandenberg AFB. Note wind sensors at 2 m and 16 m above ground.....	3
Figure 3.	Number of days per month with visibility less than 7 statute miles at Vandenberg AFB, CA (Air Force Combat Climatology Center, 2006).....	5
Figure 4.	Composite Sea-level Pressure of Western United States for month of July from 1968-1996 period of study. (From NOAA-CIRES/Climate Diagnostics Center, 2004).....	8
Figure 5.	Conceptual model of the average lower atmosphere in summer in the eastern North Pacific during periods of persistent north-northwesterly winds (from Beardsley et al. 1987).....	9
Figure 6.	Vertical cross-section of potential temperature in Kelvin (black), isotachs in m/s (blue), and cross-section winds (red). Downward vectors represent subsidence and horizontal vectors represent along cross-section winds. Cross-section oriented SW-NE near Point Arena, CA.....	10
Figure 7.	Vertical cross-section of potential temperature in Kelvin (black), isotachs in ms^{-1} (blue), and cross-section winds (red) near Big Sur, California.....	14
Figure 8.	COAMPS™ four-nested domain coverage for the simulations discussed in this thesis. Horizontal resolution for each nest domain is shown next to each window in kilometers.....	21
Figure 9.	National Data Buoy Center moored buoy locations (blue squares) across Central California. (From National Data Buoy Center 2006).....	24
Figure 10.	National Data Buoy Center moored buoy locations (blue squares) across Southern California (From National Data Buoy Center 2006).....	24
Figure 12.	Composites of NCEP GFS model 500 mb geopotential height (green), and 500 mb absolute vorticity (dashed blue) for June 20-23, 2006 analyses. All times are at 0000Z.....	27

Figure 13.	Composites of NCEP GFS model 850 mb geopotential height (green) and 850 mb wind vectors (blue) for June 20-23, 2006 analyses. All times are at 0000Z.....	29
Figure 14.	Composite of NCEP GFS model sea level pressure (green) and 1000 mb wind vectors (blue) for June 20-23, 2006 analyses. All times are at 0000Z.....	31
Figure 15.	Composite analysis of COAMPS™ model 950 mb wind speed (solid black) and wind vectors (red) for June 21-24, 2006. All times are at 0000Z. Coastal jet maximum wind axis depicted with dashed black line.....	33
Figure 16.	Vertical cross-section COAMPS™ model analysis of cross-section wind vectors (blue), potential temperature (red), and perpendicular to cross-section wind speed (black) in m/s for June 22 and June 23 at 0000Z.....	34
Figure 17.	Wind Direction (degrees) for the period June 20/00Z - June 25/00Z measured at Buoy 46011 near Santa Maria, 20 nautical miles northwest of Point Arguello, CA. The 6-hour period (June 21, 1200Z - 1500Z) during which windshift occurred is highlighted in yellow.....	35
Figure 18.	Wind speed (knots) for the period June 20/00Z - June 25/00Z measured at Buoy 46011 near Santa Maria, 20 nautical miles northwest of Point Arguello, CA. The 6-hour period (June 21, 1200Z - 1500Z) during which windshift occurred is highlighted in yellow.....	35
Figure 19.	Wind Direction (degrees) for the period June 20/00Z - June 25/00Z measured at Buoy 46028 near Cape San Martin. The 6-hour period (June 22, 0900Z - 1200Z) when windshift occurred is highlighted in yellow.....	36
Figure 20.	Wind speed (knots) for the period June 20/00Z - June 25/00Z measured at Buoy 46028 near Cape San Martin. The 6-hour period (June 22, 0900Z - 1200Z) when windshift occurred is highlighted in yellow.....	36
Figure 21.	Composite analysis of COAMPS™ model 950 mb wind speed (blue), vectors (black) and sea-level pressure (red) for June 24 at 0000Z.....	38
Figure 22.	Composite analysis COAMPS™ model 950 mb potential temperatures in Kelvin and 850 mb (mountain top) winds for June 23 at 0000Z.....	40

Figure 23.	Vertical cross-section COAMPS™ model analysis of cross-section wind vectors (blue), potential temperature in Kelvin (red), and along cross-section winds (dashed black) in m/s for June 22 at 0000Z.....	41
Figure 25.	Composite analysis of COAMPS™ model 950 mb through 700 mb thickness for 0000Z, June 20, 2006 and 0000Z, June 24, 2006.....	44
Figure 26.	Monterey, CA National Weather Service Office observed high temperatures compared to normal high temperatures for date. (Renard, 2006).....	46
Figure 27.	Composites of NCEP GFS model 500 mb geopotential height (green) and 500 mb absolute vorticity (blue) for July 16, July 18, July 20, and July 22, 2006 analyses. All times are at 0000Z.....	48
Figure 28.	Composites of NCEP GFS model 850 mb geopotential height (green) and 850 mb wind vectors (blue) for July 16, July 18, July 20, and July 22, 2006 analyses. All times are at 0000Z.....	50
Figure 29.	Composites of NCEP GFS model sea level pressure (green) and 1000 mb wind vectors (blue) for July 16, July 18, July 20, and July 22, 2006 analyses. All times are at 0000Z.....	51
Figure 30.	Composite analysis COAMPS™ model 950 mb vector winds (red) and isotachs (solid black) in m/s for July 16-19 at 0000Z. Coastal jet maximum wind axis depicted with dashed black line.....	53
Figure 31.	Vertical cross-section COAMPS™ model analysis of cross-section wind vectors (blue), potential temperature in Kelvin (red), and perpendicular to cross-section wind speed (black) in m/s for July 17 and July 19 at 0000Z.....	54
Figure 32.	Wind direction in degrees for the period July 17/00Z - July 23/00Z at Buoy 46028 near Cape San Martin. The 6-hour period (July 17, 2100Z - July 18, 0000Z) when windshift occurred is highlighted in yellow.....	55
Figure 33.	Wind speed in knots for the period July 17/00Z - July 23/00Z at Buoy 46028 near Cape San Martin. The 6-hour period (July 17, 2100Z - July 18, 0000Z) when windshift occurred is highlighted in yellow.....	56
Figure 34.	Vertical cross-section COAMPS™ model analysis of cross-section wind vectors (blue), potential temperature in Kelvin (red), and perpendicular	

	to cross-section wind speeds (black) in m/s for July 15 at 0000Z.....	57
Figure 36.	Composite analysis COAMPS™ model 950 mb potential temperatures (red) in Kelvin and 850 mb wind vectors (black) for July 18 at 0000Z....	59
Figure 37.	Comparison of 950-700 mb thickness in meters immediately offshore of the Santa Lucia near Pt Sur, California for both case studies.....	60
Figure 38.	Composite analysis of COAMPS™ model 950 mb through 700 mb thickness for July 18 at 1200Z...	61
Figure 39.	Forecaster decision aid for separation of coastal jet from the Central California coastline.....	66

LIST OF TABLES

Table 1.	The 40 vertical levels for the COAMPS™ model with layer height in millibars and feet.....	22
----------	--	----

THIS PAGE INTENTIONALLY LEFT BLANK

ACKNOWLEDGMENTS

First, and foremost, I would like to thank my family for sharing this great tour on the Monterey Peninsula with me. Jill, you kept me motivated to try my hardest and by being such a great mother to our two daughters, you gave me time to do the research and get the job done. Anna and Megan, thank you for sharing with me the simple treasures in life. Strolling along a rocky coastline and exploring sea life has been the best remedy for Graduate Student work.

I also would like to thank my thesis advisor, Dr. Wendell A. Nuss of the Department of Meteorology, Naval Postgraduate School, for the guidance and support during the development of this thesis. Being an advisor to so many students took a toll, but he always took the time out to answer and educate me along the way. Thanks to my second reader, Dr. Qing Wang, for the additional expertise on marine boundary layer applications along the California Coastline.

Thanks to Lt. Col. Cox, Maj. Kurtz and all the members of the 30th Weather Squadron at Vandenberg AFB, CA for answering my numerous questions, enlightening me on the local weather effects on space launch, and inviting me down to see the operations first-hand. I feel well-informed and hope the information contained in this thesis will help in future operations.

THIS PAGE INTENTIONALLY LEFT BLANK

I. INTRODUCTION

A. MOTIVATION

Vandenberg Air Force Base, located in Santa Barbara County, California along the central coast of California, is the third largest Air Force Base in the nation, encompassing over 98,400 acres. The base population consists of approximately 12,000 Air Force, Civil Service, contractor personnel, and military dependents. While the base comprises more than 2,000 buildings and 2,075 homes, only 15 percent of its total area is developed. The remainder provides the necessary safety buffer to preclude encroachment and protect outlying communities, Lompoc to the southeast and Santa Maria to the northeast, from the effects of any launch anomaly.

Vandenberg AFB and associated space flight activities might be described as a concentration of extremely expensive, environmentally sensitive systems. Complex, weather-sensitive requirements for ground processing, launch, and recovery operations are common. Weather-related failures and delays have a serious impact on cost, safety, and national prestige. Few Department of Defense activities could benefit so greatly from accurate site-specific weather support.

Weather is a critical part of every operation, affecting pre-launch and ground operations as well as launch and post launch. Of particular interests are the surface and low-level winds that impact many aspects of launch operations at Vandenberg AFB. Directly associated with the forecast of the wind field near Vandenberg AFB is the toxic

hazard forecast. Vandenberg AFB stores millions of gallons of highly toxic and explosive chemicals. Due to its proximity to local communities (Lompoc/Vandenberg Village), toxic hazard forecasting is the number one reason to be able to accurately understand and forecast low-level winds in and around the Vandenberg AFB complex. (30WS FRN 2006)

Strong low-level winds also have a profound effect on the movement of the mobile service tower (MST) and mobile assembly system (MAS) where maximum allowable winds, depending on azimuth direction, are commonly in the 25-35 knot range. Normally, these winds are measured by an anemometer located on a tower at 54 or 102 feet above ground. The map below shows the array of wind towers located on Vandenberg AFB.

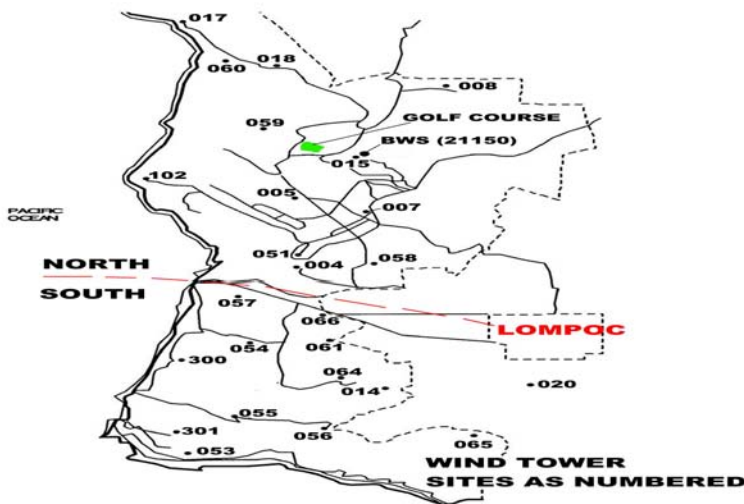


Figure 1. Map of Vandenberg AFB split into North and South region with wind tower sites denoted by number. (From 30 Weather Squadron Forecast Reference Notebook).



Figure 2. One of 26 Weather Towers located on Vandenberg AFB. Note wind sensors at 2 m and 16 m above ground.

B. VANDENBERG AFB GEOGRAPHY AND SUMMER CLIMATOLOGY

Vandenberg's unique geography provides the United States the capability to launch satellites into polar orbit without the threat of over-flying populated areas. This mission—which is crucial to our national security, as well as commercial interest in communications, land resources surveillance, and space research—is dependent on the successful launching of an imposing array of rocket boosters.

The Air Force also relies on the "window to the Pacific" to conduct operational testing of Minuteman and Peacekeeper ICBMs. These ballistic missiles are launched toward instrumented target sites near Kwajalein Atoll in the South Pacific. (30WS FRN)

Vandenberg is divided by the Santa Ynez River into two main areas, North Vandenberg (NVAFB) and South Vandenberg

(SVAFB). The airfield's geographical coordinates are (34° 44'N, 120°35'W) with a field elevation of 367 ft above mean sea level (MSL). The main base is located near the windward side of the Santa Lucia Range. (30WS FRN 2006) These relatively small mountains (1,500 ft - 6,900 ft) form an important barrier between the coast and inland valleys all along the Central Coast from just south of Monterey Bay to just north of Vandenberg AFB.

The climate of the Central Coast and Vandenberg AFB proper is characterized by mild, wet winters and warm, dry summers. The regional climate is dominated by a strong and persistent high-pressure system that frequently lies off the Pacific coast (generally referred to as the Pacific High). The Pacific High shifts northward or southward in response to seasonal changes or the presence of cyclonic storms. In its usual position to the west of Northern California, the Pacific High produces an elevated temperature inversion with a pronounced marine boundary layer. Coastal areas are characterized by southeasterly winds in the early morning, which generally shift to northwesterly later in the day. Transport of cool, humid marine air onshore by these northwest winds causes frequent fog and stratus near the coast, particularly during night and morning hours in the late spring through the summer months (Figure 3).

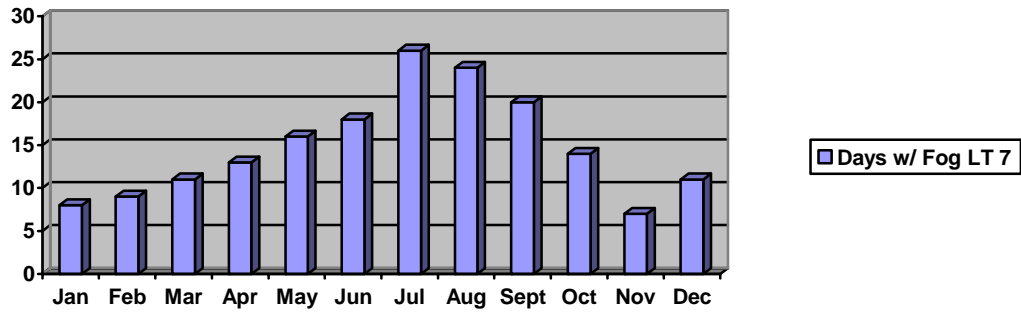


Figure 3. Number of days per month with visibility less than 7 statute miles at Vandenberg AFB, CA (Air Force Combat Climatology Center, 2006)

C. PROBLEM STATEMENT

Much emphasis has been made on the California Coastal Jet in past studies. Extensive research is available on the evolution, strength, and structure of the low-level atmospheric winds along the coast and offshore. What hasn't been researched thoroughly is how the separation of the jet from the coast occurs particularly with offshore flow. The 30th Weather Squadron at Vandenberg Air Force Base requested a method for better understanding low-level winds throughout the Vandenberg AFB complex for their unique mission of space launch. The objective of this study is to thoroughly examine the effects of offshore, cross-coast flow on the marine boundary layer and the California coastal jet and to pinpoint the trigger mechanism(s) which lead to separation of the coastal jet from the California coastline. This, in turn, will help forecast near-coast winds for numerous military operations throughout the Central California coastline but specifically for the space-launch mission at Vandenberg AFB.

THIS PAGE INTENTIONALLY LEFT BLANK

II. BACKGROUND

A. THE CALIFORNIA COASTAL JET

The California Coastal Jet is present in the lower troposphere and is driven by the pressure gradient produced by a sharp contrast between high temperatures over land and lower temperatures over the seas (Cross 2003). In the summer months, typically starting early June, a quasi-stationary eastern North Pacific high dominates the synoptic regime (Fig. 4). This high is typically centered about 1000 km west of northern California at an average latitude of 40° N (Beardsley et al. 1987). An inverted trough or thermal low often extends from the desert Southwest up the Central Valley of California to the Oregon border. These two features produce a consistent pattern of coast-parallel northwesterly winds in the lower atmosphere. The strong subsidence due to the high combined with mixing from the marine boundary layer produces a strong thermal inversion that confines the cool, moist air near the surface of the ocean.

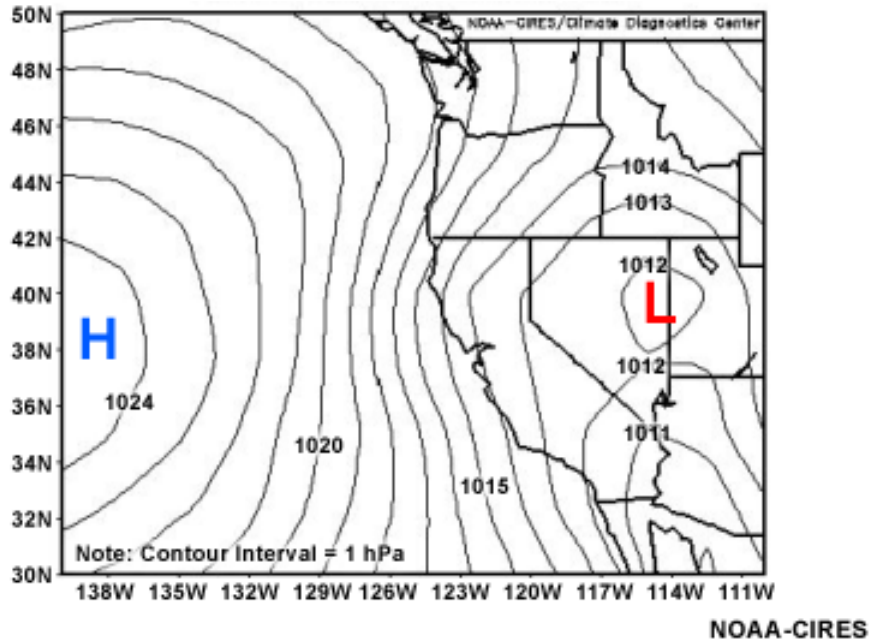


Figure 4. Composite Sea-level Pressure of Western United States for month of July from 1968-1996 period of study. (From NOAA-CIRES/Climate Diagnostics Center, 2004)

The lower atmospheric structure leading to a coastal jet starts with a cool marine boundary layer over the ocean, capped by a strong inversion. This inversion tends to slope upward offshore due to increasing sea surface temperatures (SSTs) and weakening subsidence to the west (Beardsley 1987), pictured schematically in Figure 5. Lowest SSTs of 13-15° C commonly occur at the coastline due to upwelling. Farther to the west, a dramatic increase in SST occurs beyond 20-80km, followed by a more gradual increase westward. The higher SSTs increase the heat flux from the ocean to the atmospheric boundary layer, which, combined with decreasing subsidence aloft, promotes greater vertical mixing in the boundary layer with increased distance from the coast. The combination of greater heating from below and reduced subsidence from above results in a downward sloping inversion base toward the

coast (Cross 2003). This downward sloping inversion is the key contributor to the coastal jet's location and is further described in Figure 5.

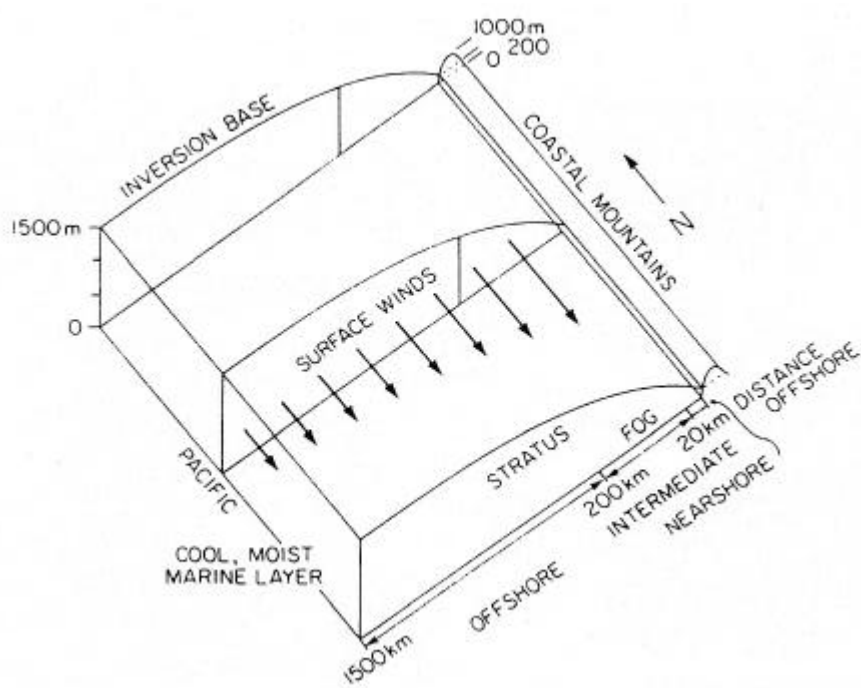


Figure 5. Conceptual model of the average lower atmosphere in summer in the eastern North Pacific during periods of persistent north-northwesterly winds (from Beardsley et al. 1987).

Figure 6 taken from the COAMPS™ 9 km model on 20 June 2006 at 0000Z, shows a typical cross-coast cross section of wind speed and isentropes with the right side of the diagram immediately onshore near Point Arena, California. This region typically experiences a relative wind speed maximum due to the steep terrain immediately onshore.

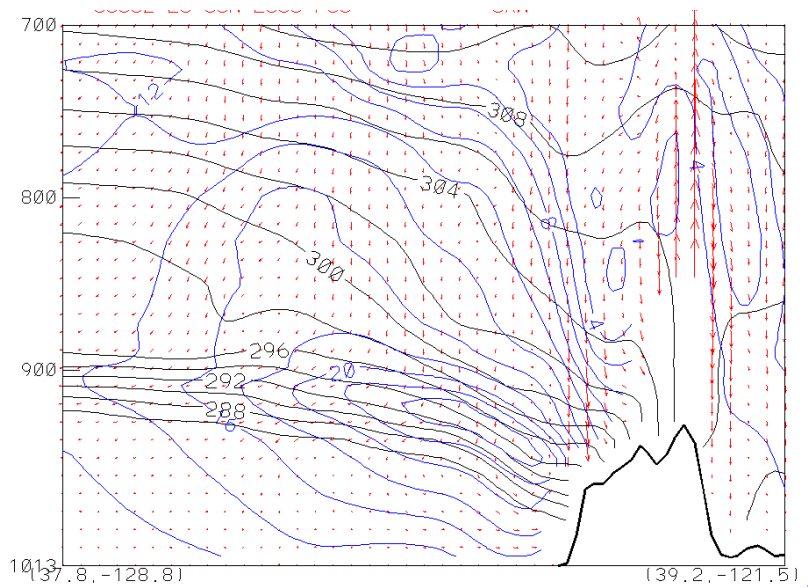


Figure 6. Vertical cross-section of potential temperature in Kelvin (black), isotachs in m/s (blue), and cross-section winds (red). Downward vectors represent subsidence and horizontal vectors represent along cross-section winds. Cross-section oriented SW-NE near Point Arena, CA.

The westward limit of the horizontal axis in Figure 6 is approximately 500 km offshore. The vertical axis is the air pressure extending from surface to 700 mb. The key features this diagram illustrates are the downward sloping isentropic surfaces (in black) towards the coast and the proximity of the strongest coast parallel winds (isotachs in blue) corresponding to the tightest potential temperature gradient at the immediate coast. In this

example the strongest winds were at approximately 925 mb or approximately 2500 ft above sea-level and are located just below the inversion near the top of the marine boundary layer. The maximum modeled winds of 25 ms^{-1} from the north-northwest in the jet core are relatively strong considering that the typical maximum wind speed of the coastal jet ranges between $15\text{-}25 \text{ ms}^{-1}$.

Given the strong daytime heating of the land surface onshore causing low pressure and the slowing of the surface winds due to friction over the ocean, one would expect at least a small component of ageostrophic, onshore flow from high to low pressure. However, due to the presence of a strong low-level inversion, the coastal mountains along most of the California Coast act as a blocking mechanism to this sea breeze component of the flow. Subsequently, this ageostrophic component of the flow turns down the coast towards lower pressure. Along the California coast, relatively lower pressure typically lies to the south, so the ageostrophic flow acts to increase the magnitude of the coastal northerly flow. Thus, coastal mountains help keep the flow oriented parallel to the coastline and suppress most of the sea breeze component that might develop. Suppression of the cool sea breeze helps to maintain the strong temperature and pressure gradient across the coast. These temperature gradients easily exceed $20\text{-}25$ degrees Celsius between the cool coastal region and the warmest inland valleys.

B. VARIATIONS IN THE CALIFORNIA COASTAL JET

Typical wind speed in the California coastal jet during the summer months is in the 15-25 ms^{-1} range hugging the Northern and Central California coastline as far south as Point Conception. Variations of the California coastal jet were observed multiple times throughout the summer season of 2006. The normal position along coast was interrupted with periods from 2-10 days where the core of the maximum speed of winds would position well offshore from the Central California coastline, sometimes as far as 500 kilometers offshore. This separation from the coastline of the coastal jet resulted in benign wind conditions along the coast or even a coastally trapped wind reversal. The frequency of these events, and the potential impacts to numerous operations, led us to examine the causes of these variations.

1. Variations in Intensity

Previous studies by Zemba and Friehe (1987) during the Coastal Ocean Dynamics Experiment (CODE) showed that the diurnal development and intensity of the coastal jet was a result of differential land-sea heating from the warm inland valleys where normal summertime temperatures easily exceed 35°C to the cool Pacific Ocean which rarely exceeds 17°C. The strength of the jet was approximated well by the thermal wind relationship, with the jet core located in the sloping marine inversion layer within one Rossby radius of deformation from the coastline.

The observed wind and potential temperature fields seen in this study are consistent with the geostrophic adjustment of a thermally direct circulation due to the strong horizontal temperature contrast between the ocean and continent. The sloping marine inversion can be interpreted as a near-geostrophic frontal boundary between the cool maritime and the warmer continental air. The scale of the sloping marine boundary layer is consistent with that expected due to geostrophic adjustment. The sloping marine inversion near the coast is responsible for the stronger winds near the coast where the strongest temperature and pressure gradient is colocated. The movement westward of the strongest gradient then, in effect, should also move the strongest core of coastal jet winds westward. This is exhaustively studied in subsequent chapters.

2. Variations in Location

As mentioned above, results from CODE 1987 suggest the coastal jet extends over a horizontal scale on the order of the Rossby radius of deformation. If one assumes an inversion strength of 5-15 K and a marine boundary layer height of 500 m, the Rossby radius of deformation is approximately 100-150 km. This is consistent with what has been noted in previous studies and what was seen as the preconditions to our offshore events during the summer of 2006.

A sloping marine boundary layer offshore from the coastline was present for all of the days preceding our case studies in 2006. An example is shown in Fig. 7 using

COAMPS simulations on 21 June 2006 at 0000Z off the coast of the Santa Lucia mountain range. Here the depth of the boundary layer increased from less than 500 meters near the coast to greater than 1500 meters at the west end some 500 km away.

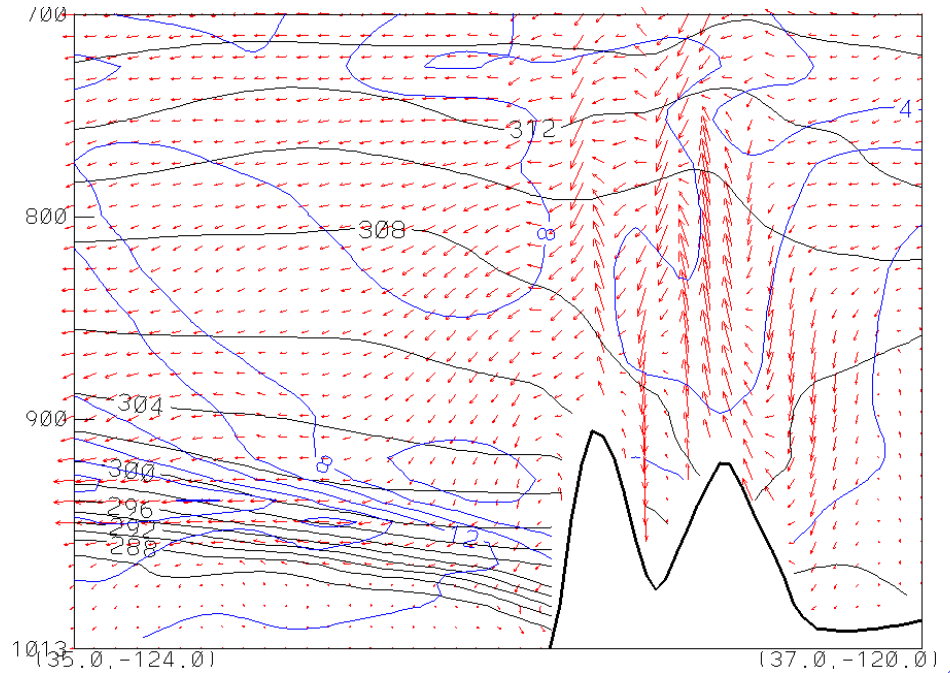


Figure 7. Vertical cross-section of potential temperature in Kelvin (black), isotachs in ms^{-1} (blue), and cross-section winds (red) near Big Sur, California.

It is suggested that the offshore increase in the marine boundary layer depth is the result of geostrophic adjustment in the cross-coast direction due to the pronounced thermal gradients at the coast. The differential heating between ocean and land forces a thermally direct circulation that results in a sloping frontal structure of the marine boundary layer, separating the cool maritime air from the warm continental air. Horizontal temperature gradients and hence a thermal wind

result from this adjustment process and are responsible for the rapid decrease in wind speed about the inversion.

As seen throughout our case studies, which will be discussed in much further detail in subsequent chapters, the core maximum wind speeds are located where the frontal structure of the marine boundary layer has its greatest slope. When the greatest slope of the marine boundary layer is separated from the coast and transported offshore, the coastal jet also moves westward.

C. POSSIBLE CAUSES OF COASTAL JET VARIATIONS

1. Synoptic-scale Features

The typical synoptic-scale regime during the summer months positions a quasi-stationary eastern North Pacific 500 mb high pressure ridge approximately 1000 km west of northern California. An inverted trough or thermal low at lower-levels, usually from surface to 850 mb, often extends from the desert Southwest up the Central Valley of California to the Oregon border. These two features produce a consistent pattern of northwesterly winds in the lower atmosphere.

A synoptic component which may play a major role in offshore flow development and the migration of the coastal jet is the location of the 850 mb to 500 mb high pressure region. When high pressure at these levels becomes more northeasterly tilted or migrates to the northeast closer to the Pacific Northwest coastline, the pressure gradient force becomes more northeasterly, or offshore, along the central California coastline.

At lower levels, typically from 850 mb to 700 mb, high pressure migrating to the central California coastline near the San Francisco Bay would produce a broad region of low to mid-level subsidence and suppress the marine boundary layer near the coastline. A broad region of the suppressed boundary layer near coast would flatten the isentropic surfaces where typically there is a steep slope due to the strong horizontal thermal gradient. Weaker subsidence further west would relax the boundary layer, resulting in a steeper slope of the marine boundary layer from east to west located further west. This synoptic scale horizontal pressure gradient in the low to mid-levels is in direct correlation to the position of the strongest coastal jet winds and their distance from the coast.

Another possible synoptic-scale trigger mechanism for offshore winds along the Central California coast during the summer months is a thermal trough at low levels migrating westward towards the Southern California coast in the form of an easterly wave. The thermal trough would then be positioned to the south of the high pressure region causing a more northeasterly pressure gradient force thus a cross-coast wind versus a northwest coast-parallel wind. This westerly drift of the thermal trough coupled with the area of high pressure migrating to the northeast towards the Oregon coastline would enhance the offshore winds. These synoptic-scale trigger mechanisms leading to offshore winds and possible westward migration of the coastal jet will be investigated further in forthcoming chapters.

2. Downsloping Wind Compression of the Boundary Layer

When the offshore component of the winds is set up synoptically, a significant amount of cross-mountain flow is induced across the coastal mountain ranges that make up the majority of the coastline of California. Depending on the directional component of the winds, often times these offshore winds are perpendicular to the northwest-southeast running Santa Lucia range. General theory and observational analysis suggest that downsloping winds occur on the lee side of a mountain range when upstream synoptic-scale flow becomes perpendicular to the mountain ridge axis and terrain blocking is not present. However, terrain characteristics cannot be the sole explanation for downsloping winds. The varying atmospheric stability is a contributing factor as well. During our case studies, the stable environment is present only downstream from the mountain range. Offshore winds were often located at the level of the inversion above the marine boundary layer top, which is normally below the mountain top. These conditions are favorable for downslope wind events or a "foehn" development. Foehn winds are a warm, dry, downsloping wind descending on the lee side of a mountain range as a result of synoptic-scale, cross-barrier flow over the mountain range. The air achieves its warmth and dryness due to adiabatic descent on the lee side of the mountain range. This downsloping wind exhibits strong influence on the top of the marine boundary layer. The majority of past studies on downslope wind events ignored the characteristics of the marine boundary layer.

Assuming the marine boundary layer to be rigid is erroneous as the marine boundary layer is very complex. Jiang et al (2002) demonstrated that a stable or stagnant boundary layer acts as a sponge layer to trapped waves and downsloping winds and partially absorbs downgoing wave energy. As a result, the lee-wave amplitude decays exponentially with downstream distance. In general, the decay coefficient increases with increasing surface roughness, that is, downsloping winds decay faster over a rougher surface. It is found that the decay coefficient is very sensitive to surface heat flux. With surface cooling, the decay coefficient could be significantly increased, which implies that a nocturnal boundary layer or a summertime marine boundary layer, where the surface heat flux is negative or downward, is more efficient in absorbing wave energy and damping trapped waves. This leads to the impact of downsloping wind compression on the marine boundary layer limited to immediately along the California coastline downstream from the coastal mountain ranges. This compression of the marine boundary layer due to downsloping winds tends to flatten the isentropic surfaces near the coast. When compression further westward diminishes significantly, the slope of the marine boundary layer inversion increases from east to west. This will be discussed in greater detail in subsequent chapters.

III. DATA ANALYSIS

Synoptic events that resulted in offshore flow over most of the Central California coast were selected for this study for the time period between late spring and early fall in 2006. A total of 18 events were found. Typical intervals between the events are about 7 days in late Spring and increase gradually to about 10 days in late Summer to early Fall due to building high pressure in the Great Basin after landfalling cold fronts associated with mid-latitude cyclones. Two case studies were selected from the 18 events by examining the cross-coast offshore winds, length of duration, the degree of marine boundary layer compression, and coastal jet westward migration. These two events exhibited normal preconditions where the coastal jet hugged the coastline from the Oregon/California border south toward Point Conception. At the early stages of these events, the large-scale low-level flow, usually between 950 mb up to 500 mb, turned to offshore. The two days selected for extensive analyses both had cross-coast components in their 950 mb to 500 mb flow, usually 010-140 degrees azimuth, and lasted a minimum of 48 hours. Results are described in Chapter IV.

A. DATA

1. Atmospheric Model

Comparing with the limited number of observations, output from a mesoscale model is ideal to get sufficiently fine vertical resolution to explore the lower atmospheric

structure, to provide a large-scale background of coastal jet tendencies, and to shed light on the complex flow interaction with coastal topography. The model used in this study is COAMPS™, as trademarked by the Naval Research Laboratory (NRL) and described by Hodur (1997). COAMPS™ is run twice a day by NRL with a 3 km horizontal resolution as its inner nest of four nests and 40 vertical levels. A fine vertical resolution is achieved, particularly in the lowest 1000 m (boundary layer) of the atmosphere, where the vertical resolution is every 10 mb. The COAMPS™ model is initialized with the three-dimensional NRL Atmospheric Variational Data Assimilation System (NAVDAS), capable of taking full advantage of the myriad of remotely-sensed meteorological observations currently available and planned for the future. NAVDAS was designed to effectively exploit these non-conventional observations and, thus, improve the forecast performance of the Navy's atmospheric prediction systems. (NRL, 2003)

The model was run with four nests as shown in Fig. 8. The outermost nest has a spatial resolution of 81 km with the next nest a spatial resolution of 27 km. The next inner nest used most frequently in this study covers the central California coast with a spatial resolution of 9 km and the innermost nest over the San Francisco Bay and Monterey Bay region has a resolution of 3 km. The inner nest boundary conditions are interpolated from the next outer grid. COAMPS™ was initialized by NAVDAS on 40 vertical levels (Table 1). Due to the interest in the mesoscale behavior of the lower atmosphere, the distribution of these levels was set to be dense near the surface and less dense in the upper atmosphere. The lowest

σ level is at the surface, followed by the second level at 10 m above the surface, followed by one every 10 mb up to 890 mb. Above 890 mb, the vertical resolution becomes 25 mb up to 400 mb and then 50 mb spacing to the model top (100 mb). The model was run with the standard set of parameterizations used by the Navy operationally, as described in Hodur (1997).

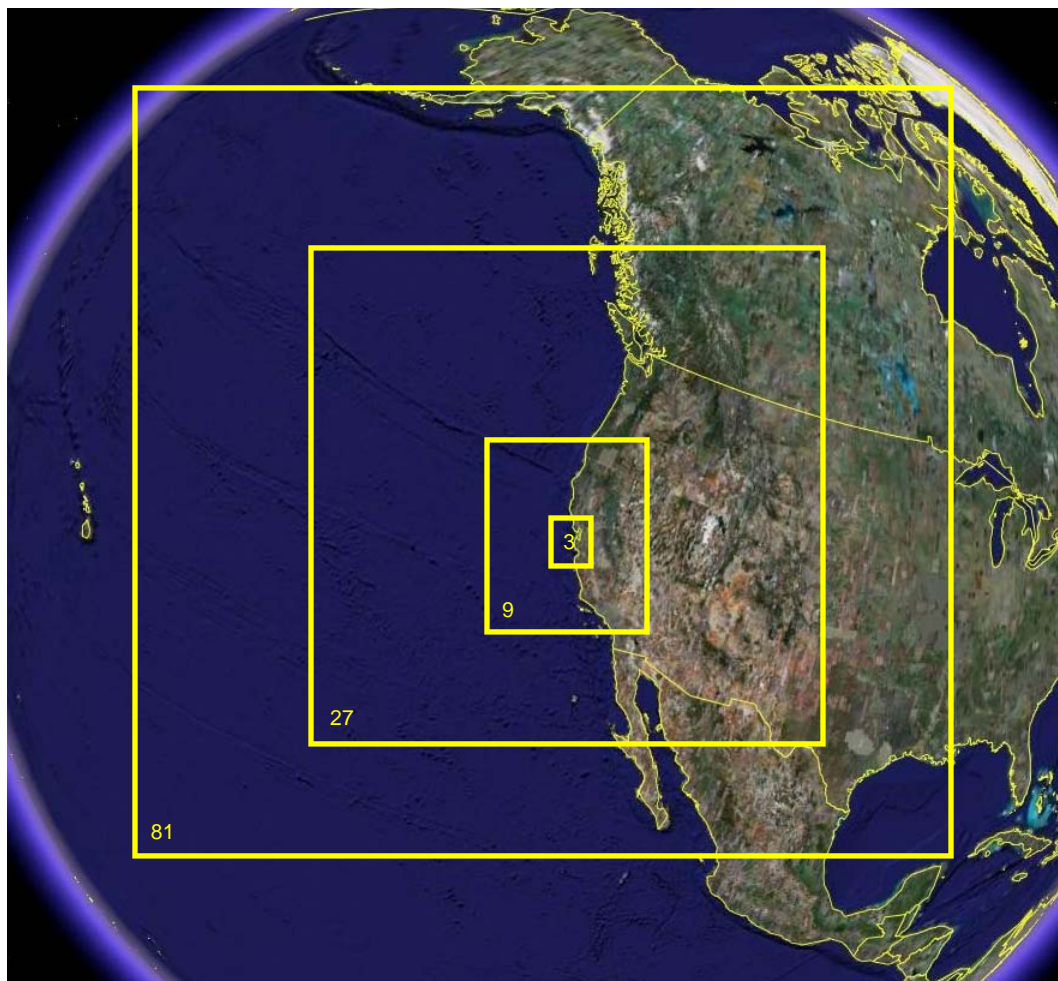


Figure 8. COAMPS™ four-nested domain coverage for the simulations discussed in this thesis. Horizontal resolution for each nest domain is shown next to each window in kilometers.

σ	Layer height (mb)	Layer height (ft)	σ	Layer height (mb)	Layer height (ft)
1	SFC	0	21	725	9000
2	1010	30	22	700	10,000
3	1000	300	23	675	11,000
4	990	600	24	650	11,750
5	980	900	25	625	12,750
6	970	1200	26	600	13,750
7	960	1500	27	575	15,000
8	950	1750	28	550	16,000
9	940	2000	29	525	17,000
10	930	2300	30	500	18,250
11	920	2600	31	475	19,500
12	910	2900	32	450	21,000
13	900	3200	33	425	22,000
14	890	3500	34	400	23,500
15	875	4000	35	350	26,500
16	850	4750	36	300	30,000
17	825	5500	37	250	34,000
18	800	6250	38	200	38,000
19	775	7250	39	150	43,000
20	750	8000	40	100	48,000

Table 1. The 40 vertical levels for the COAMPS™ model with layer height in millibars and feet.

2. National Data Buoy Center Buoy Observations

NDBC provides hourly observations from a network of about 90 buoys and 60 Coastal Marine Automated Network (C-MAN) stations to help meet observational needs in a data-sparse region. All stations measure wind speed, direction, and gust, barometric pressure, and air temperature. In addition, all buoy stations, and some C-MAN stations,

measure sea surface temperature and wave height and period (NDBC 2006). While the moored buoys by the National Data Buoy Center along the California Coast are placed at similar distances offshore (Figs. 9 & 10), they exist in a variety of locations relative to coastal features. For example, Buoys 46026 and 46042 are adjacent to the openings of San Francisco Bay and Monterey Bay, respectively, while Buoy 46014 is close to the steep topography north of Point Arena. Buoy 46028 (Cape San Martin, south of Point Sur) is particularly well located to represent the extension at the surface of coastal jet winds aloft. While it is potentially in the lee of Point Sur (modeled position of the jet maximum varies relative to buoy location), the coastal characteristics in that area are reasonably representative of the average coastline, and its location is somewhat farther offshore than the other buoys, which places it farther from the direct effects of coastal friction and land/sea breeze circulations.

The COAMPS™ model output was compared with available in situ data such as the National Data Buoy Center observations to confirm that the models mesoscale structure is generally consistent with the observations. This was done for all the analysis time periods used in the study up to the 12 hour forecast only. With confidence in the model results thus established, a range of inferences have been made relative to the evolution of the coastal marine boundary layer and associated coastal jet winds during these two offshore events using the model data only.

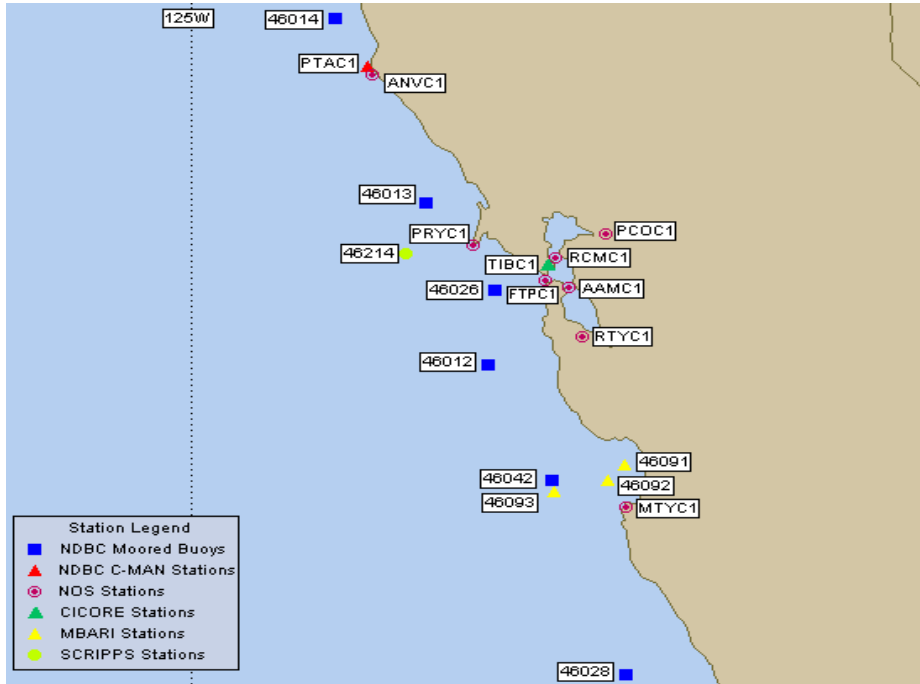


Figure 9. National Data Buoy Center moored buoy locations (blue squares) across Central California. (From National Data Buoy Center 2006)

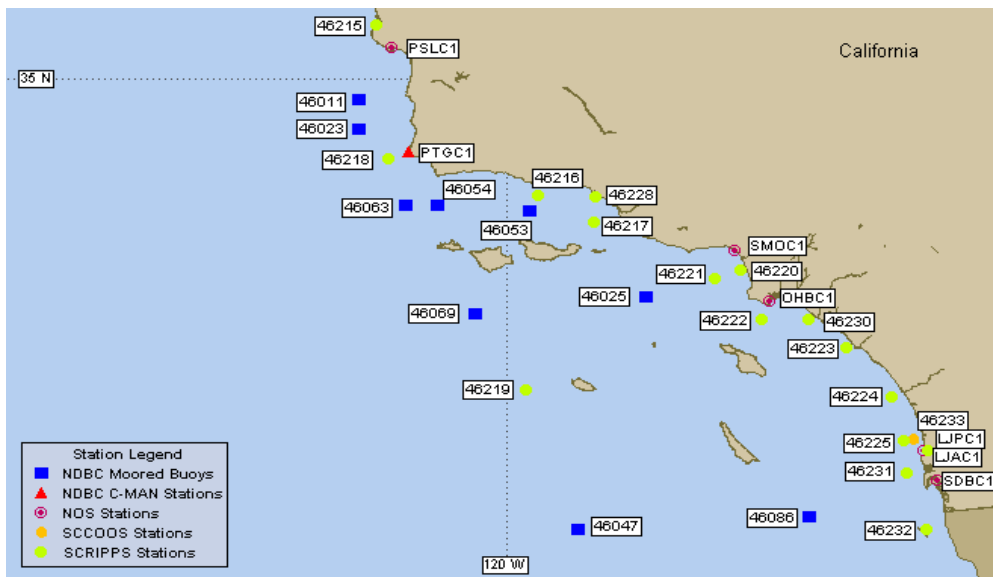


Figure 10. National Data Buoy Center moored buoy locations (blue squares) across Southern California (From National Data Buoy Center 2006)

IV. RESULTS

Two offshore wind events during the summer of 2006 were selected from 18 events using the duration of cross-coast wind and the degree of coastal jet separation from the coastline as criteria. The first case occurred June 20-24, 2006 and began with coastal jet features very typical for a summertime regime off the California coast. Compared with other events throughout the summer it was moderate in length lasting approximately 100 hours. The second case study was a month later occurring July 16-24. This was much longer in duration than any of the offshore events witnessed during the summer of 2006. It was also a record producer in terms of coastal temperature readings. Numerous reporting stations near the Central Coast, including Monterey and Santa Maria, reported record high temperatures for 3-5 consecutive days between July 20-25. These high temperatures were 15°F to as much as 25°F above normal.

A. JUNE 20-24, 2006

1. Synoptic Overview

Initially, on June 20 at 0000Z, there is southwesterly flow in between a 5460 dam, 500 mb Gulf of Alaska low centered at 52N, 152W and a 5940 dam, 500 mb High centered at 37N, 152W (Fig. 12a). The 500 mb ridge axis is located just offshore with a positive tilt and a minor 500 mb trough directly over Central California causing the southwesterly flow located throughout the Northeast Pacific

to veer to a more northwesterly direction closer to the California coastline. With a weak 500 mb trough axis over the region at this point, the typical mid-level subsidence is replaced with an area of positive absolute vorticity yielding to rising motion in the mid-levels.

On June 21-22 (Figs. 12b,c), the 500 mb trough has shifted to the east with increasing subsidence being introduced to central California by the 500 mb ridge to the west. By June 23, the 500 mb trough in the Northeast Pacific has moved south shifting the Eastern Pacific ridge to the east over central California, Sierra Nevada and the Nevada basin (Fig. 12d). The main impact of this 5940 dam 500 mb high is a large area of subsidence directly over the central California coastline. Geopotential heights increased across central California from 5850 dam on June 20 to 5940 dam on June 23. The location of the 500 mb high also gives light southwesterly flow to the north of the San Francisco Bay region and easterly offshore flow at mid levels to areas south of San Francisco.

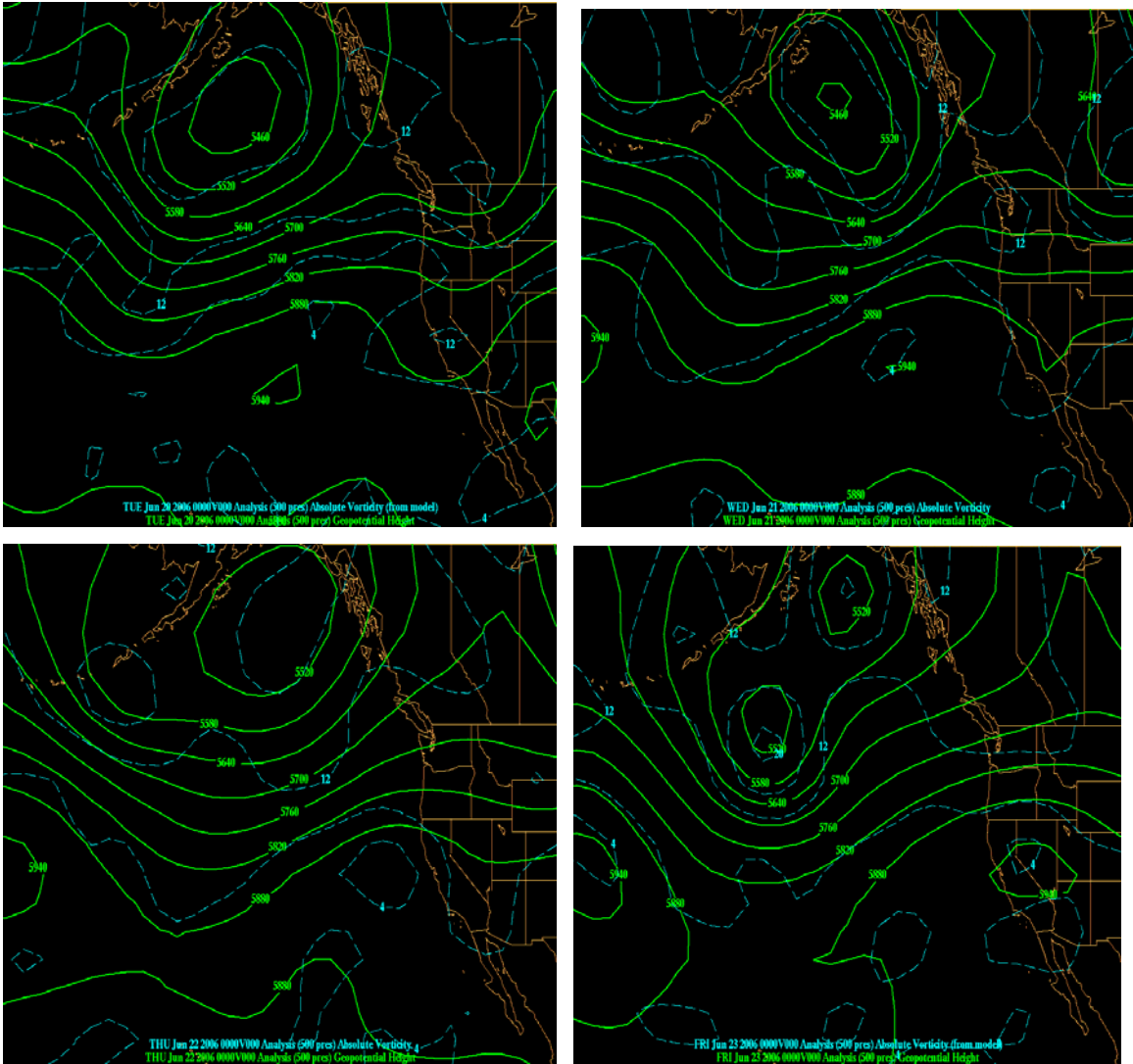


Figure 12. Composites of NCEP GFS model 500 mb geopotential height (green), and 500 mb absolute vorticity (dashed blue) for June 20-23, 2006 analyses. All times are at 0000Z.

At 850 mb on June 20 (Fig. 13a), strong high pressure is elongated in a southwest to northeast direction with the ridge axis nosing itself to just offshore of the Washington coast. The 850 mb high is vertically stacked under the 500 mb high and a tight north to south pressure gradient force

is located along the West Coast between the 850 mb high and the 850 mb thermally induced low in the southwest United States. This tight gradient along the California coastline is leading to 850 mb north-northwesterly winds of 30-40 knots typically seen this time of year. During the next several days the 850 mb ridge moves slightly to the northeast and weakens from 1620 dam to 1590 dam (Figs. 13b-d). The main 850 mb evolution that impacts the low-level wind in the region is the westward drift of the thermal trough that was located near New Mexico and Colorado on June 20. The 24-hour period between June 22 at 0000Z (Fig. 13c) and June 23 at 0000Z (Fig. 13d) exhibited the strongest 850 mb offshore gradient due to the 850 mb ridge migrating southeast over central California and the thermal trough holding firm over the desert SW. This 24-hour period will be the focus on this case study. North-northeast winds of 20-25 knots at 850 mb were analyzed by the GFS model throughout the central coast on June 22.

By June 23, the thermal trough has undercut the 850 mb ridge and is located offshore of Southern California (Fig. 13d). This position of a thermal trough offshore has given the majority of Central California a northeasterly, offshore flow of 10-20 knots at 850 mb.

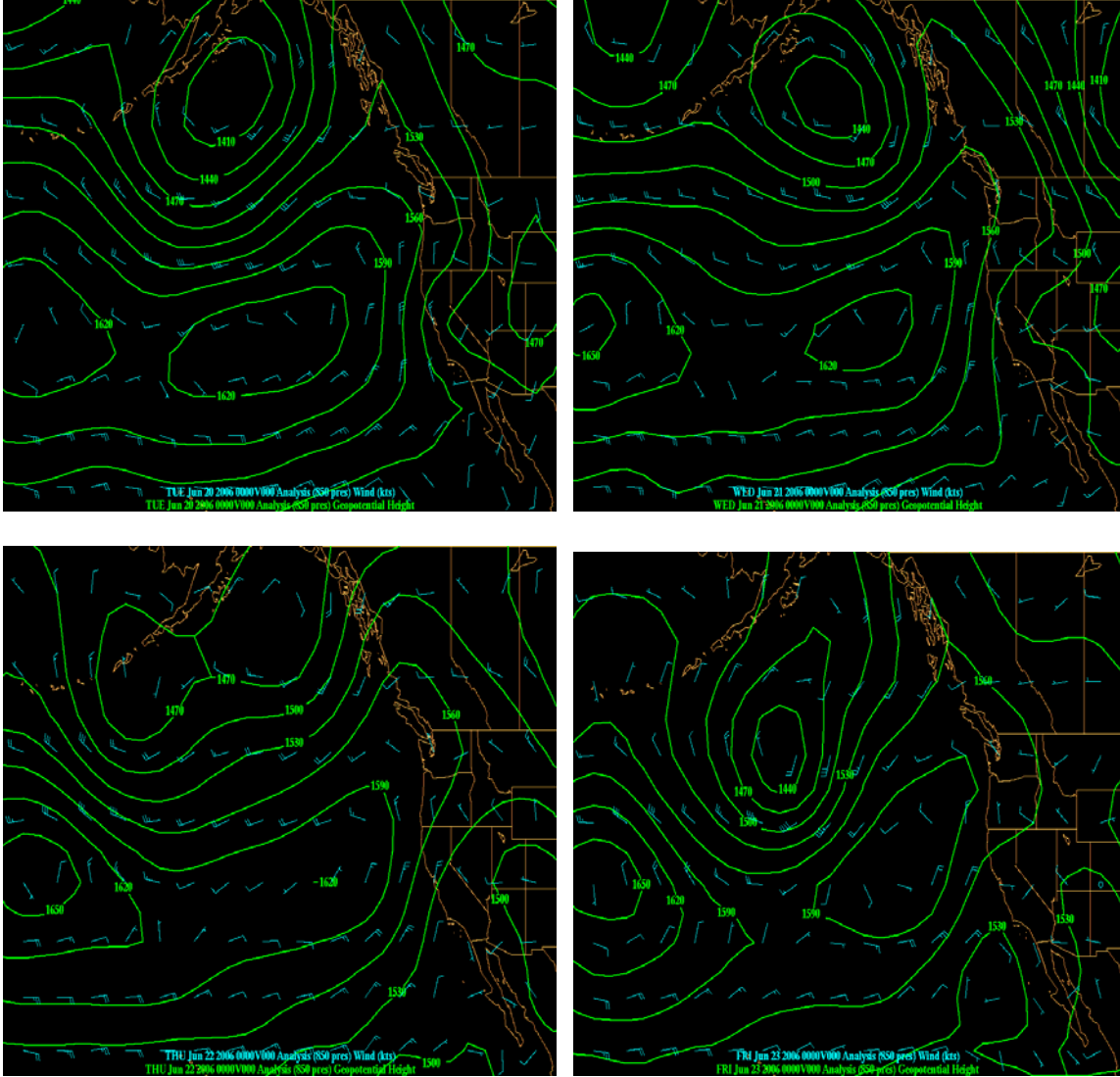


Figure 13. Composites of NCEP GFS model 850 mb geopotential height (green) and 850 mb wind vectors (blue) for June 20-23, 2006 analyses. All times are at 0000Z.

At the surface on June 20, the 1033 mb high pressure is located approximately 400 nm off the Northern California coastline with a northeasterly positively tilted ridge axis approaching the Washington coastline (Fig. 14a). The surface thermal trough is centered over much of the Southwestern desert with a weak trough axis over the

Nevada/California border. The pressure gradient throughout California is parallel with the coastline early in the period of this study with the strongest gradient near Point Arena approximately 200 nm north of the Monterey Bay area. 1000 mb GFS June 20, 0000Z analysis shows 15-30 knot northwesterly winds directly offshore indicative of a mature coastal jet.

By June 23, similar to what occurred at 850 mb, the surface high pressure weakened slightly to 1031 mb and the ridge axis was oriented slightly more northeast to just offshore of the Washington coastline (Fig. 14d). Again, the main mechanism influencing low-level flow was the westward drift of the thermal trough reorienting the pressure gradient force to offshore, northeasterly flow. Surface pressure along the California coastline only dropped slightly but the pressure gradient shifted from a northerly to a northeasterly flow by June 23 due to the trough axis now located near the San Joaquin Valley of California. The pressure gradient loosens considerably along the central coast with GFS analysis 1000 mb winds light and variable.

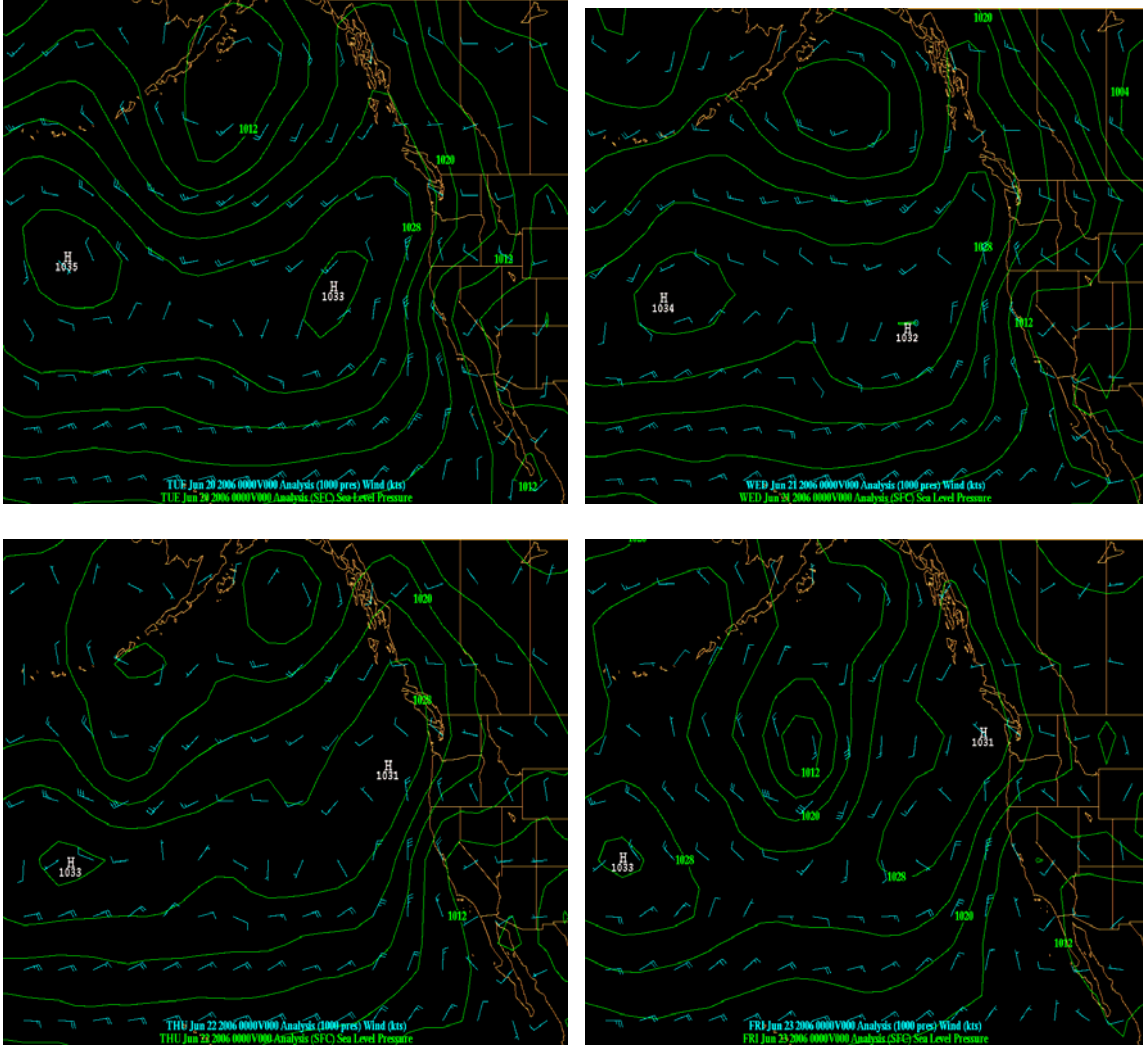


Figure 14. Composite of NCEP GFS model sea level pressure (green) and 1000 mb wind vectors (blue) for June 20-23, 2006 analyses. All times are at 0000Z.

2. Coastal Jet Migration

Initially, on 20 June at 0000Z, the coastal jet exhibited typical location and structure for the summertime season. Maximum model winds reached at 950 mb were a strong 30 m/s downstream from Point Arena where a local maximum is often located because of expansion fan hydraulics (Fig. 15a). In fact, strong coastal jet winds at 950 mb were seen within

100 km of the coast as far south as Point Conception near the mouth of the Santa Barbara channel with a northwesterly wind component throughout the entire region. By June 21, the coastal jet has begun its displacement to the west, especially from Monterey Bay southward where the winds are now north-northeast and offshore (Fig. 15b). In Figure 15, the axis of strongest winds has been outlined in a dashed black line. The initial displacement of the jet began June 21 approximately 0000Z-1200Z. The maximum winds associated with the coastal jet moved offshore dramatically through the course of the event with the largest displacement occurring between 22 June at 0000Z and 23 June at 0000Z. As previously mentioned, this was the time frame the coast experienced the strongest offshore flow at 850 mb. By June 24 at 0000Z, the entire coastal jet has been displaced from the coast with the southern portion of the jet approximately 250 km from the coast. 950 mb winds along the entire coastal jet are now northeasterly at 18-22 m/s showing a windshift of 60-90 degrees.

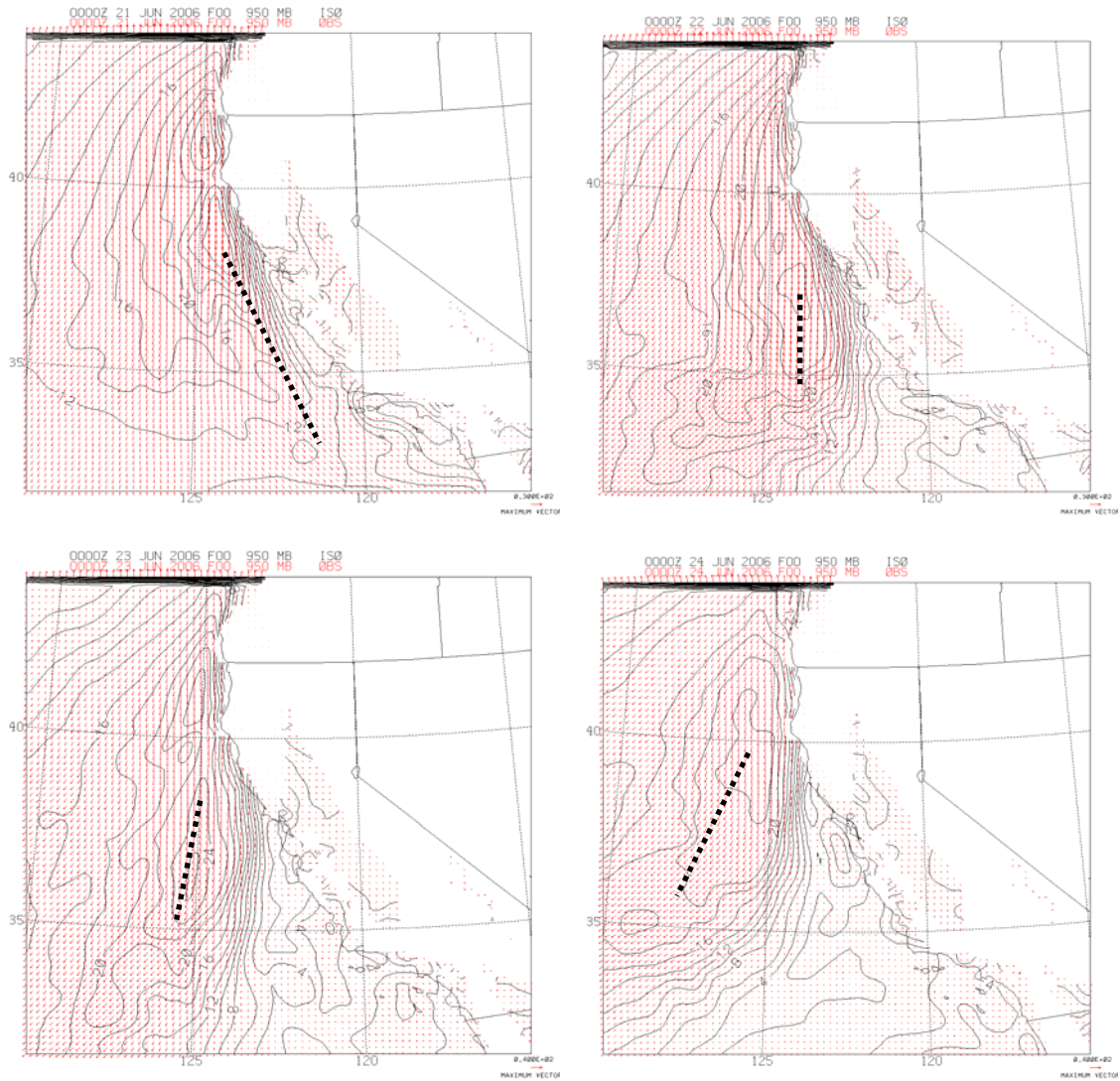


Figure 15. Composite analysis of COAMPS™ model 950 mb wind speed (solid black) and wind vectors (red) for June 21-24, 2006. All times are at 0000Z. Coastal jet maximum wind axis depicted with dashed black line.

A comparison of two cross-sections just offshore of the Santa Lucia along the central coast is shown in Figure 16. Here the most dramatic shift of the coastal jet is seen on the lee side of the Santa Lucia. At 0000Z on June 22, the jet core at 950 mb has a maximum wind of 16-20 m/s and are located immediately offshore. Twenty-four hours

later (June 23 at 0000Z), wind speeds at the same location reduced to only 4 m/s with the jet core winds shifted approximately 300 km to the west.

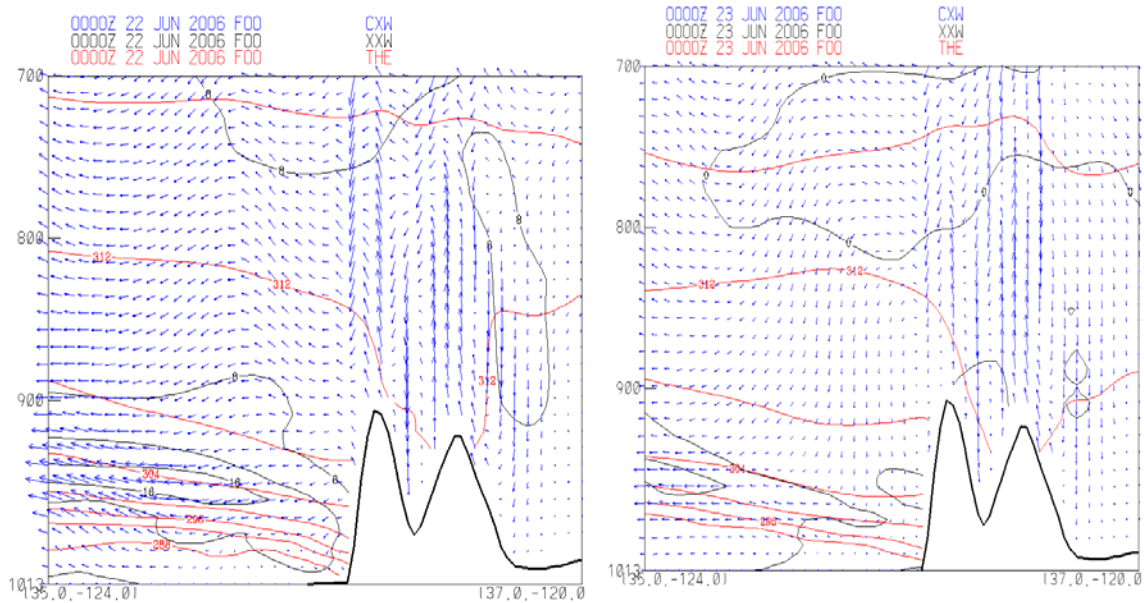


Figure 16. Vertical cross-section COAMPS™ model analysis of cross-section wind vectors (blue), potential temperature (red), and perpendicular to cross-section wind speed (black) in m/s for June 22 and June 23 at 0000Z.

The shift of the jet core westward was also verified by measurements at Buoy 46028 at Cape San Martin (Figs. 17 & 18) located 55NM WNW of Morrow Bay west of the Santa Lucia range and at Buoy 46011 near Santa Maria (Figs. 19 & 20) 20 nm northwest of Point Arguello, CA. Initially, at both buoy locations, winds are northwesterly at 4-6 m/s. As seen in Figures 17 & 19, it is obvious Buoy 46028, and Buoy 46011 are being influenced by the coastal jet until the sudden change in direction on 21 June at 1200Z for buoy 46011 and 24 hours later for buoy 46028.

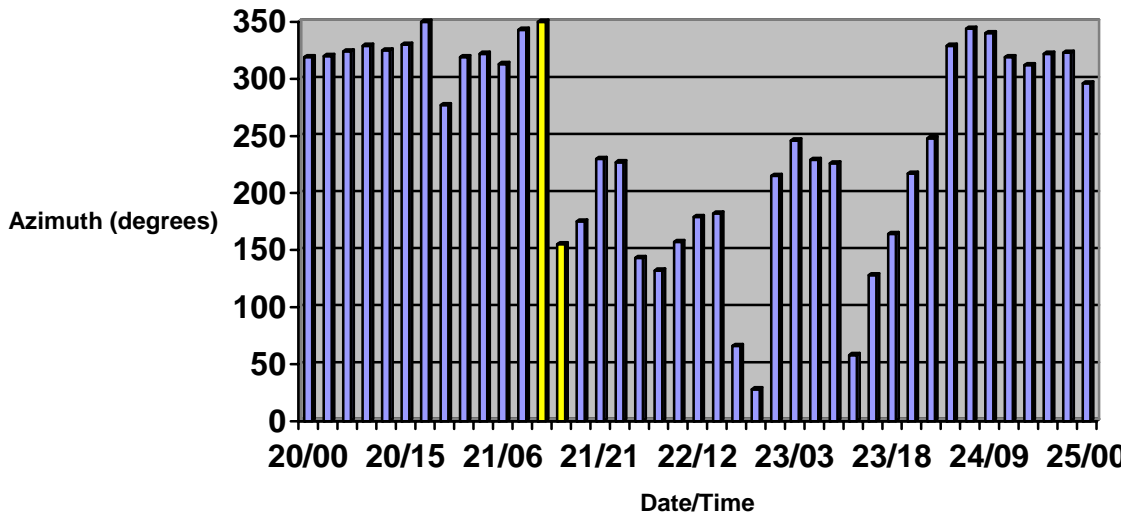


Figure 17. Wind Direction (degrees) for the period June 20/00Z - June 25/00Z measured at Buoy 46011 near Santa Maria, 20 nautical miles northwest of Point Arguello, CA. The 6-hour period (June 21, 1200Z - 1500Z) during which windshift occurred is highlighted in yellow.

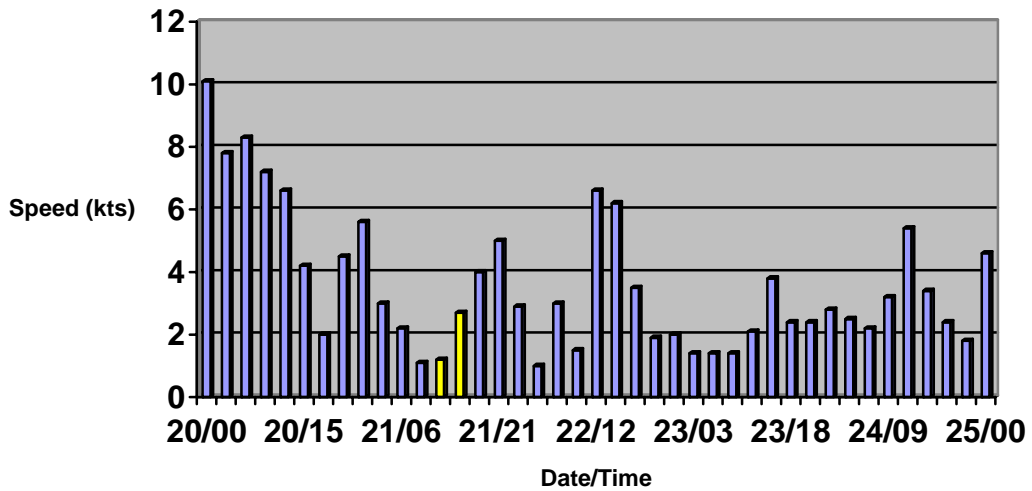


Figure 18. Wind speed (knots) for the period June 20/00Z - June 25/00Z measured at Buoy 46011 near Santa Maria, 20 nautical miles northwest of Point Arguello, CA. The 6-hour period (June 21, 1200Z - 1500Z) during which windshift occurred is highlighted in yellow.

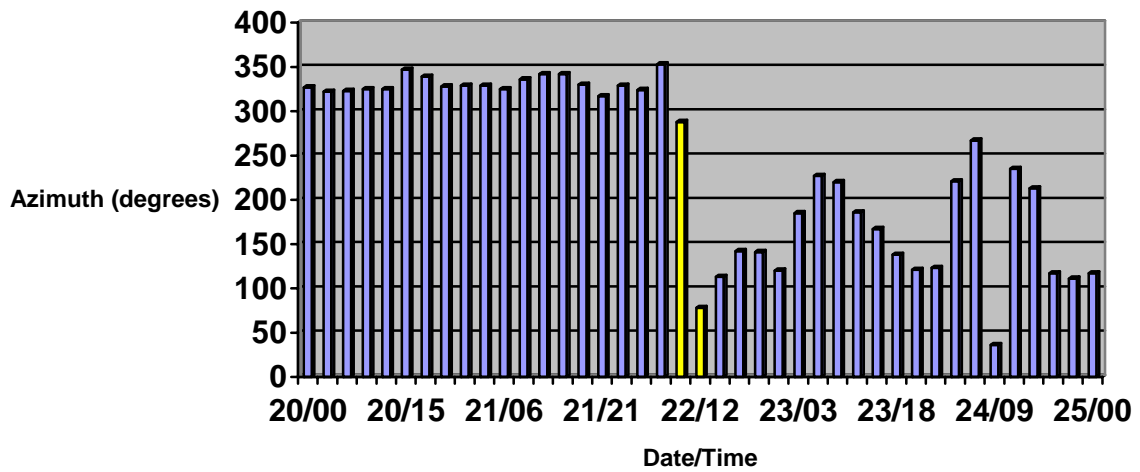


Figure 19. Wind Direction (degrees) for the period June 20/00Z - June 25/00Z measured at Buoy 46028 near Cape San Martin. The 6-hour period (June 22, 0900Z - 1200Z) when windshift occurred is highlighted in yellow.

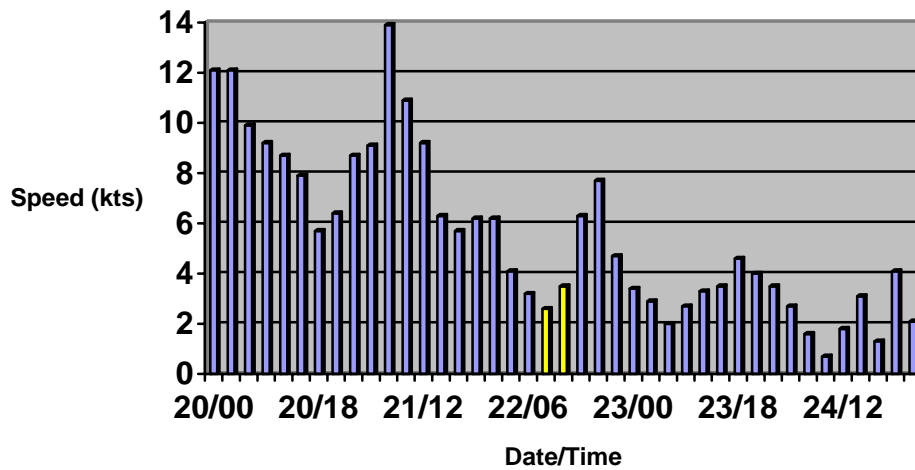


Figure 20. Wind speed (knots) for the period June 20/00Z - June 25/00Z measured at Buoy 46028 near Cape San Martin. The 6-hour period (June 22, 0900Z - 1200Z) when windshift occurred is highlighted in yellow.

On June 24 at 0000Z (Fig. 15d), the coastal jet showed the furthest displacement from coastal California. This is also the period when the strongest offshore wind began to diminish. At this time, the jet was near the coast north of Point Arena but actually moved SSW from Point Arena to approximately (35°N, 130°W). The jet indeed weakened from 96 hours prior but maintained its core wind strength of 15-20 m/s. The real significant changes in wind strength were felt at 950 mb immediately offshore of the central California coast particularly downstream from the Santa Lucia mountain range. Approximately 96 hours prior, the model winds were typically 10-15 m/s, but decreased to 2 m/s by June 24 at 0000Z (Fig. 21).

During the 48-72 hours of the coastal jet progressing to the west-northwest, the eastern edge of the North - South aligned jet was always placed at where the sea level pressure gradient started to show signs of relaxing. This shows that the coastal jet at 950 mb, or immediately above the inversion, is influenced by the placement of the surface high pressure to the northwest and the area of surface low pressure immediately off the coast of Southern California. This alignment of the coastal jet also shows it is in geostrophic balance.

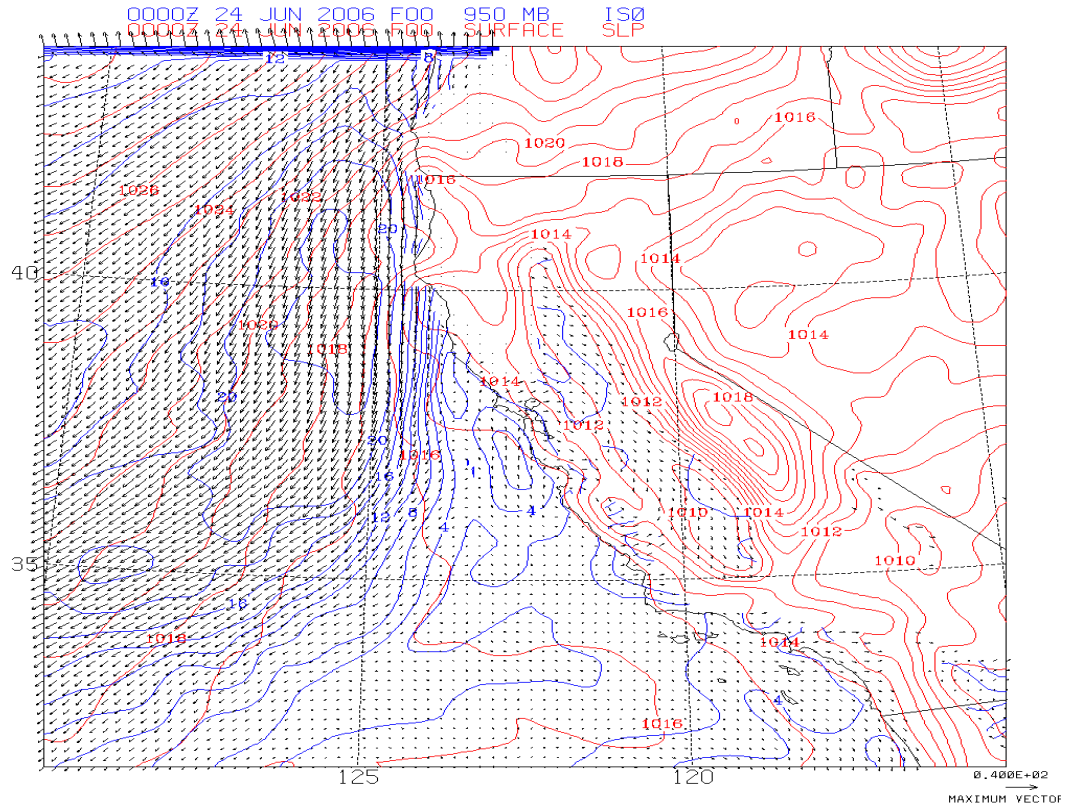


Figure 21. Composite analysis of COAMPS™ model 950 mb wind speed (blue), vectors (black) and sea-level pressure (red) for June 24 at 0000Z.

3. Marine Boundary Layer Changes

The largest change in boundary layer height occurred between June 20 at 1200Z to June 21 at 1200Z throughout the Central Coast. Initially, before the strong offshore flow setup, the top of the boundary layer was approximately 910 mb or just below mountain top. This represents a reasonably deep marine boundary layer of approximately 970 m. Within 24 hours, the boundary layer compressed to approximately 580 m. As expected, the core coastal jet wind maxima also increased the most at this time. On June 20 at 1200Z northerly winds were at 14 m/s. This increased

to 24 m/s as the coastal jet maxima moved from south of Point Arena to offshore of Point Sur.

This 24-hour period of decrease in boundary layer height correlates extraordinarily well with the largest low to mid-level geopotential height increase seen throughout the case study. On June 20 at 0000Z, as mentioned in the synoptic section, there is a weak 500 mb trough over the region with 500 mb heights approximately 5860 dam leading to minimal subsidence. By June 21 at 0000Z, the 500 mb heights increased to approximately 5900 dam with an increase of subsidence along the entire central coast. The ridge axis at all levels up to 500 mb was positioned just offshore of the Central California Coast. This resulted in onshore flow in Northern California and offshore flow in Central and Southern California. Twenty-four hours later, during the strongest low to mid-level offshore gradient, a few features are worth noting. When analyzing the 950 mb contour plot of theta surfaces to show the topology near the top of the boundary layer along with mountain top wind flow, we found higher potential temperatures at 950 mb almost always occurring just southwest (downstream) of the larger coastal mountains along the Central Coast, the Santa Lucia. This is indicative of the marine boundary layer being compressed immediately downstream of higher terrain where downsloping winds are occurring. Also, at 950 mb, the lowest potential temperatures occurred downstream of the Monterey Bay and Morrow Bay where there is lack of steep terrain near the coast, no downsloping winds, and lack of compression of the boundary layer.

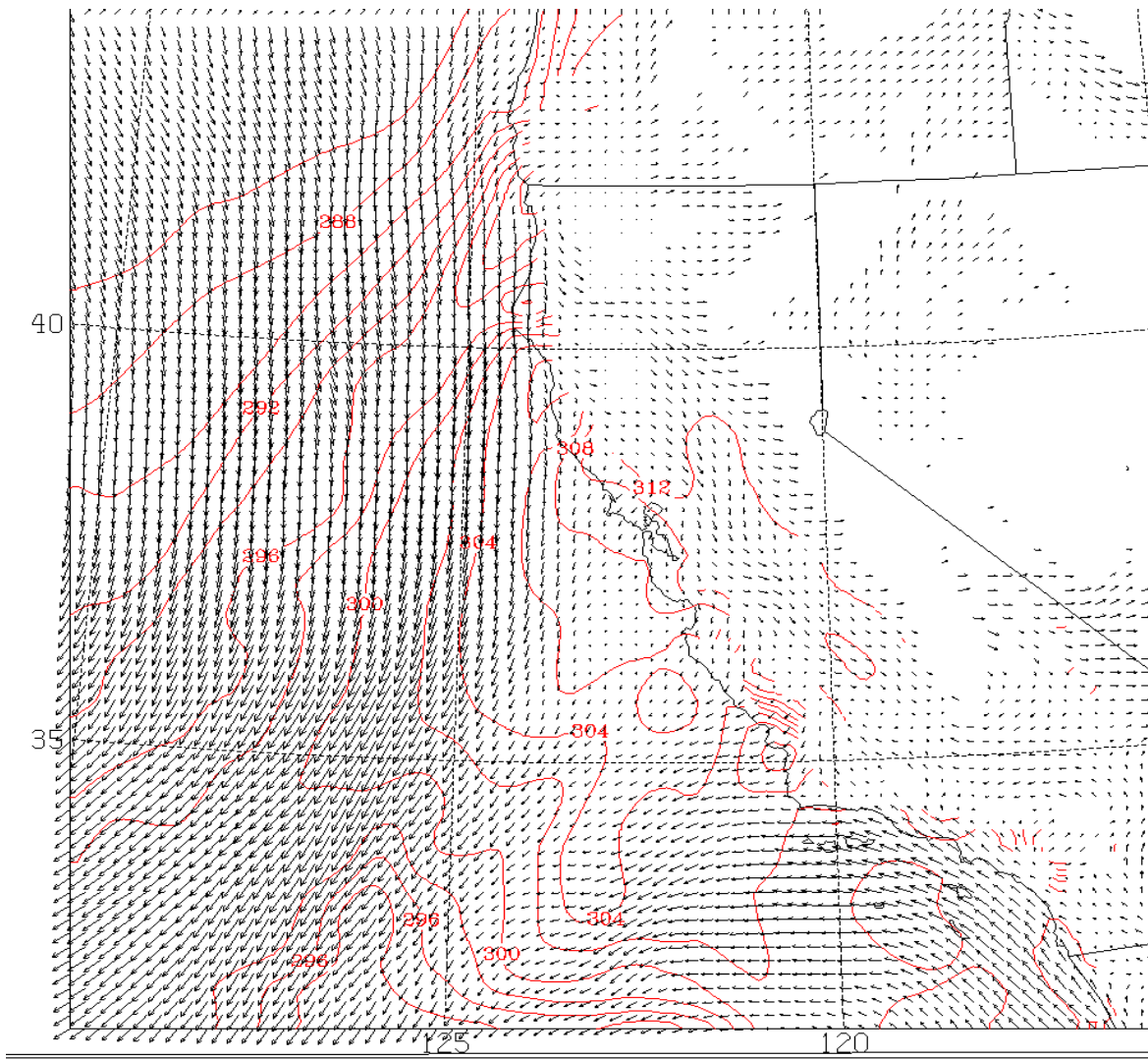


Figure 22. Composite analysis COAMPS™ model 950 mb potential temperatures in Kelvin and 850 mb (mountain top) winds for June 23 at 0000Z.

The broad region of subsidence centered north near the San Francisco Bay led to a large-scale compression of the marine boundary layer during the 24-hour period of June 20 at 1200Z to June 21 at 1200Z. But looking at the 950 mb potential temperature we find a large horizontal variability in potential temperatures at the top of the boundary layer. This signals there are also mesoscale effects of compressional warming and downsloping winds on

the boundary layer near where the steepest terrain is closest to the Pacific.

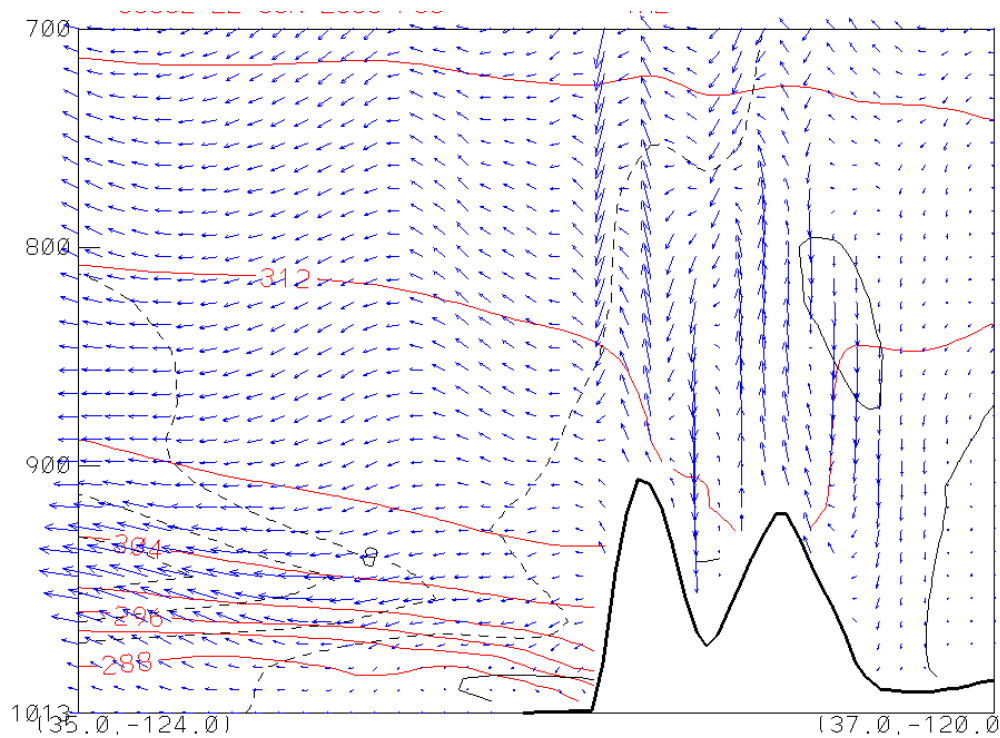


Figure 23. Vertical cross-section COAMPS™ model analysis of cross-section wind vectors (blue), potential temperature in Kelvin (red), and along cross-section winds (dashed black) in m/s for June 22 at 0000Z.

On June 22 at 0000Z, the beginning of the strongest period of offshore winds, cross-mountain flow at mountain crest, as shown in Fig. 23, was only 2-4 m/s but accelerated on the leeside of the Santa Lucia especially near the top of the boundary layer inversion. Winds approximately 100 km offshore were 8-12 m/s, an order of 3-4 times stronger than at mountain crest. Due to the compression of the boundary layer when this warming at 950 mb occurred, and the subsidence marginally increasing downstream from the Santa Lucia, compressional warming from cross-mountain flow is occurring and is exhibiting signs of

down-sloping winds. Other possible reasons for the warming at 950 mb immediately above the boundary layer would be horizontal warm air advection from the California interior immediately upstream from the Santa Lucia where 0000Z temperatures were near 38C. This was ruled out because if horizontal warm air advection from interior California across the Santa Lucia was the only mechanism occurring, the boundary layer would not be compressed as we saw during this period. The effects of horizontal warm air advection alone would be to increase the temperature gradient across the inversion.

4. June 20-24 Summary

The major cause of the shift in the coastal jet during this event was due to subsidence just offshore along the entire central coast. The 950-700mb thickness, as seen in Figure 24, increases throughout the period downstream from the Santa Lucia from 2580 meters June 20 at 0000Z to 2645 meters June 24 at 1200Z. The largest increase in thickness occurred during June 21 when thickness values increased from 2600 meters at 0000Z to 2635 meters on June 22 at 0000Z. This correlates strongly with the start of the migration of the coastal jet to the west as seen in Figure 15.

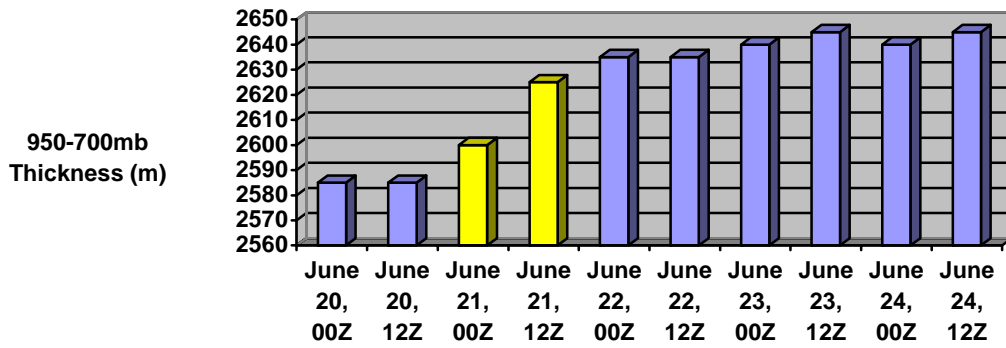


Figure 24. 950-700 mb thickness in meters immediately offshore of the Santa Lucia near Pt Sur, California during June 20-24.

Both mechanisms, the movement of the horizontal pressure gradient from east to west and mesoscale downsloping wind caused the marine boundary layer top to become more sloped from east to west and to separate the coastal jet from the California coast. This steepness from west to east of the boundary layer top has, through thermal wind balance, acted as an eastern border to the winds shifting the jet maximum westward 300 km.

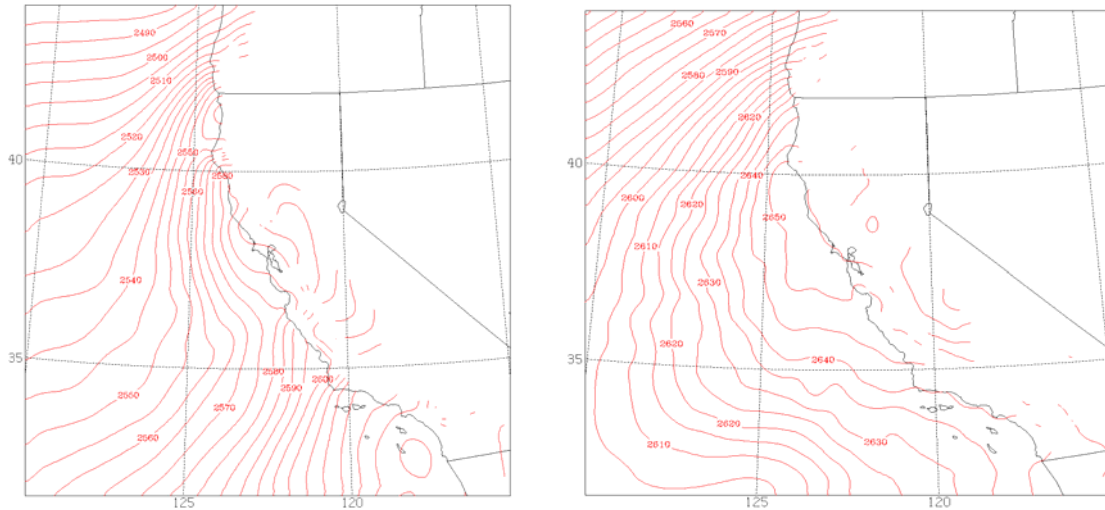


Figure 25. Composite analysis of COAMPS™ model 950 mb through 700 mb thickness for 0000Z, June 20, 2006 and 0000Z, June 24, 2006.

The northeastward migration of the Pacific High at low to mid-levels and the lowering of sea-level pressure off of the Southern California coast was also a contributing factor to the separation of the jet from the coastline. This caused the surface pressure gradient to displace offshore and the coastal jet shifted north to south and eventually, toward the end of the period, north to southwest away from land. During this time, however, the offshore winds had a tendency to compress the boundary layer at locations where flow was over steep terrain. This produced localized areas downstream of higher terrain with a more compressed boundary layer due to lee-side downsloping wind flow over the terrain. These downsloping winds didn't travel more than 100-200km downstream due to weak horizontal winds (U) but also strong absorption of the winds by the marine boundary layer.

B. JULY 16-24, 2006

The second offshore event studied occurred a month later and had many similarities to the first one discussed in the previous section. A well defined coastal jet was positioned directly offshore throughout the Central Coast prior to the onset of offshore winds. The major difference between the two case studies was the strength and direction of the offshore winds and the amount of low to mid-level subsidence and its role on the evolution of the coastal jet. More detailed analysis on these two features will be discussed later. The offshore winds were initiated by the cross-coast gradient between an 850 mb high moving northeast towards the Oregon and Washington coastline and a thermal trough at low-levels in the desert Southwest shifting westward closer to the Southern California coastline. This event lasted for one week, much longer than the previous one. It also produced record high temperatures for most of coastal California. High temperatures throughout the region, particularly along the central coast were well above average, with four consecutive days of record temperatures (July 21-24) recorded by the Monterey National Weather Service Office. (Renard, 2006)

**Monterey, CA National Weather Service Office High
Temperatures vs Normal**

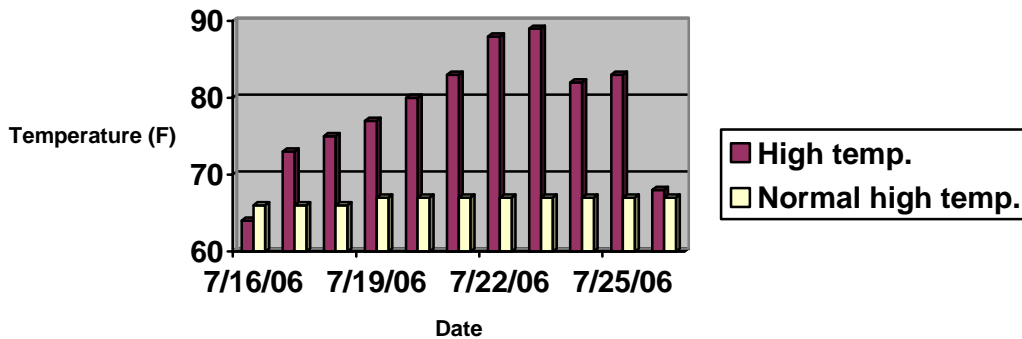


Figure 26. Monterey, CA National Weather Service Office observed high temperatures compared to normal high temperatures for date. (Renard, 2006)

1. Synoptic Overview

A 500 mb trough on July 16, 000Z was approximately 750 km offshore of the Pacific Northwest giving west-southwest 500 mb flow to much of the West Coast (Fig. 27a). The strong 500 mb high centered over Colorado with geopotential heights of 597 dam at 0000Z on July 16 is the dominant large scale feature for this case study. Throughout the following 96 to 120 hours, the meridional pattern increases with a strong 500 mb ridge throughout the intermountain west. By July 22 at 0000Z, (Fig. 27d) a blocking pattern has developed along the western half of the United States with a massive 600 dam 500 mb high retrograding and centering itself over Northern Utah with the ridge axis north-northwestward into Central British Columbia. In fact, Salt Lake City, Utah had the highest 500 mb height (599 dam) recorded among all their 1200 UTC soundings between 1998 and 2006, while the 500 mb heights at other

stations in the southwestern United States were between the 91st and 97th percentile for 1200 UTC July soundings (Maxwell, 2007). 500 mb heights across central California actually remain consistent throughout the period at approximately 594 dam (Figs. 27a-d). The only changes are the orientation of the 500 mb pressure field and associated vertical motion. Southwesterly flow and upward vertical motion occurred ahead of the trough on June 16 while southeasterly flow and subsidence occurred on June 22 due to the retrograding high pressure.

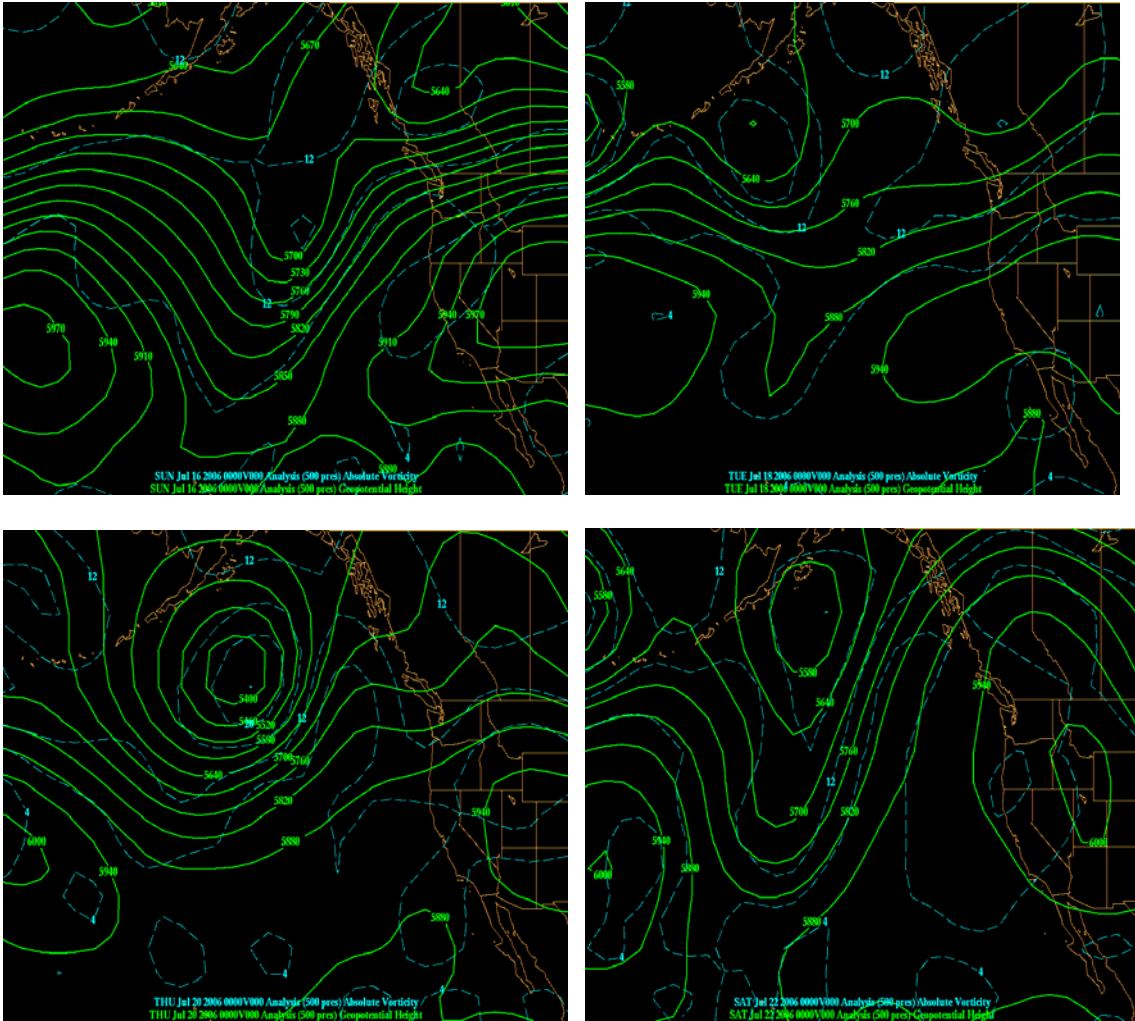


Figure 27. Composites of NCEP GFS model 500 mb geopotential height (green) and 500 mb absolute vorticity (blue) for July 16, July 18, July 20, and July 22, 2006 analyses. All times are at 0000Z.

At 850 mb on July 16 at 0000Z (Fig. 28a), we see a strengthening center of high pressure just offshore from central California with heights of 156 dam. The placement of this feature and its position to the thermal trough in the southwest United States will again be the trigger of offshore flow for much of Central California as it builds

and orients itself from the southwest to the northeast just off the Washington coast giving cross-coast flow to much of central California. In this case study, contrary to the June event, 850 mb flow at the early stages is rather light with July 18, 0000Z GFS analysis (Fig. 28b) showing only 5-10 m/s. As will be shown later, this doesn't mean there is not a strong coastal jet feature in place. The marine boundary layer is much more compressed in this event and strong coastal jet winds are evident below 900 mb and especially at 950 mb.

By July 20, 0000Z (Fig. 28c), slight offshore flow along Central California is beginning to form due to the 850 mb high building to the northeast. This slight move to the northeast has veered the 850 mb winds from a 350 direction to a 030 direction from the San Francisco Bay area northward. We are also seeing a thermally induced weakness in the 850 mb height field along the desert southwest moving slightly westward. Offshore winds at 850 mb along the central coast never exceed 5 m/s on any analysis throughout the 7-day period, proving the lack of offshore winds contribution effects to the marine boundary layer. Light winds at 850 mb on July 22 (Fig. 28d) have actually veered to the southeast similar to 500 mb and are translated upward through the entire column to 300 mb as the Utah ridge intensifies. A thermal trough feature is still evident along the Colorado River valley north to Idaho.

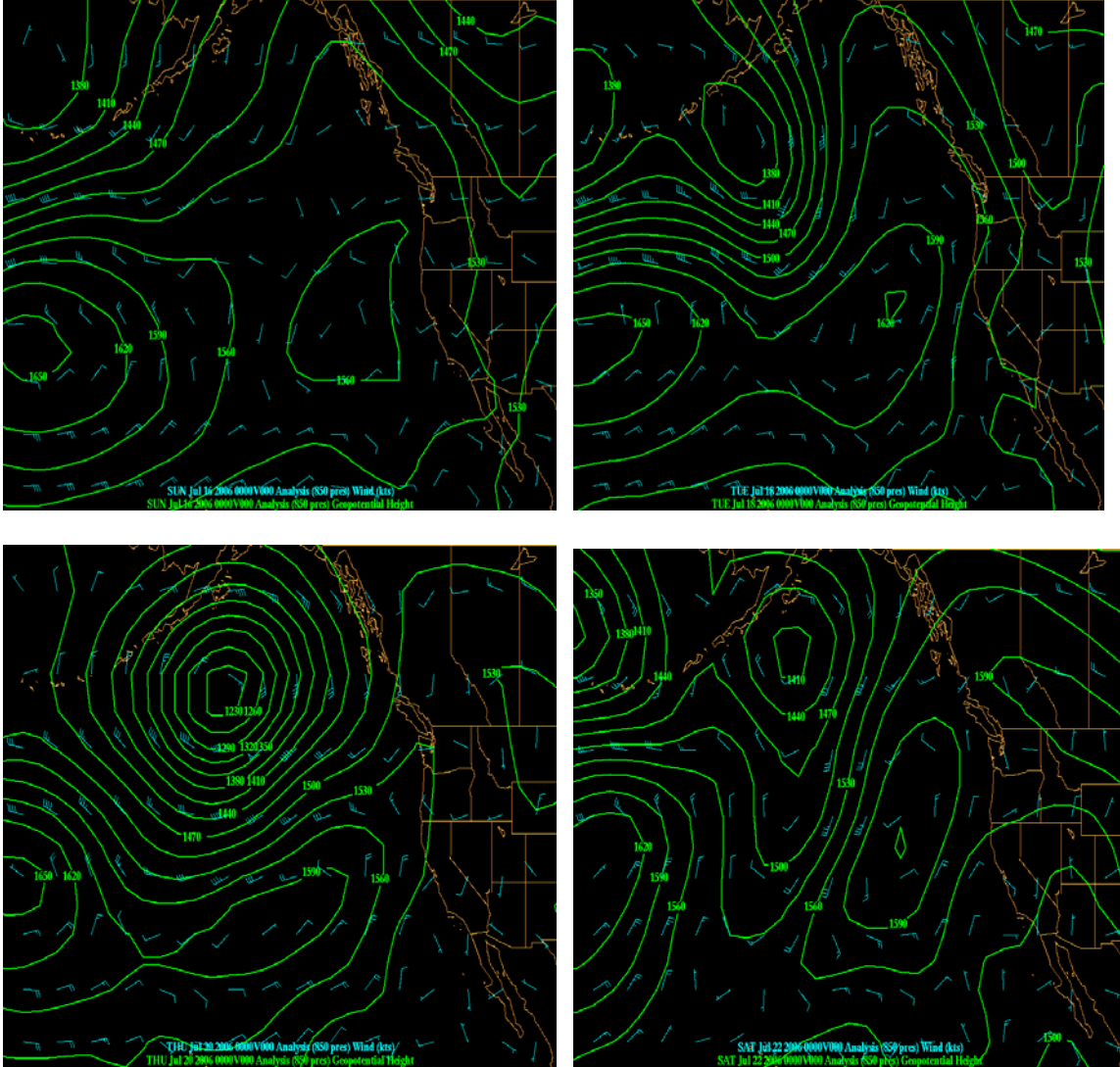


Figure 28. Composites of NCEP GFS model 850 mb geopotential height (green) and 850 mb wind vectors (blue) for July 16, July 18, July 20, and July 22, 2006 analyses. All times are at 0000Z.

At the surface, high pressure of 1027 mb maintains its strength and position off the northern California and Oregon coastline throughout the period (Fig. 29). The main evolving feature is the deepening of the thermal low in the interior desert of Southern California. On July 16 (Fig. 29a), the central low pressure of the thermal low was near

1008 mb but lowered to 1003 mb by July 22 (Fig. 29d). This strengthening of low pressure increases the gradient slightly throughout the period along the central coast. The main feature, though, with this case study is the lack of a pressure gradient at any level.

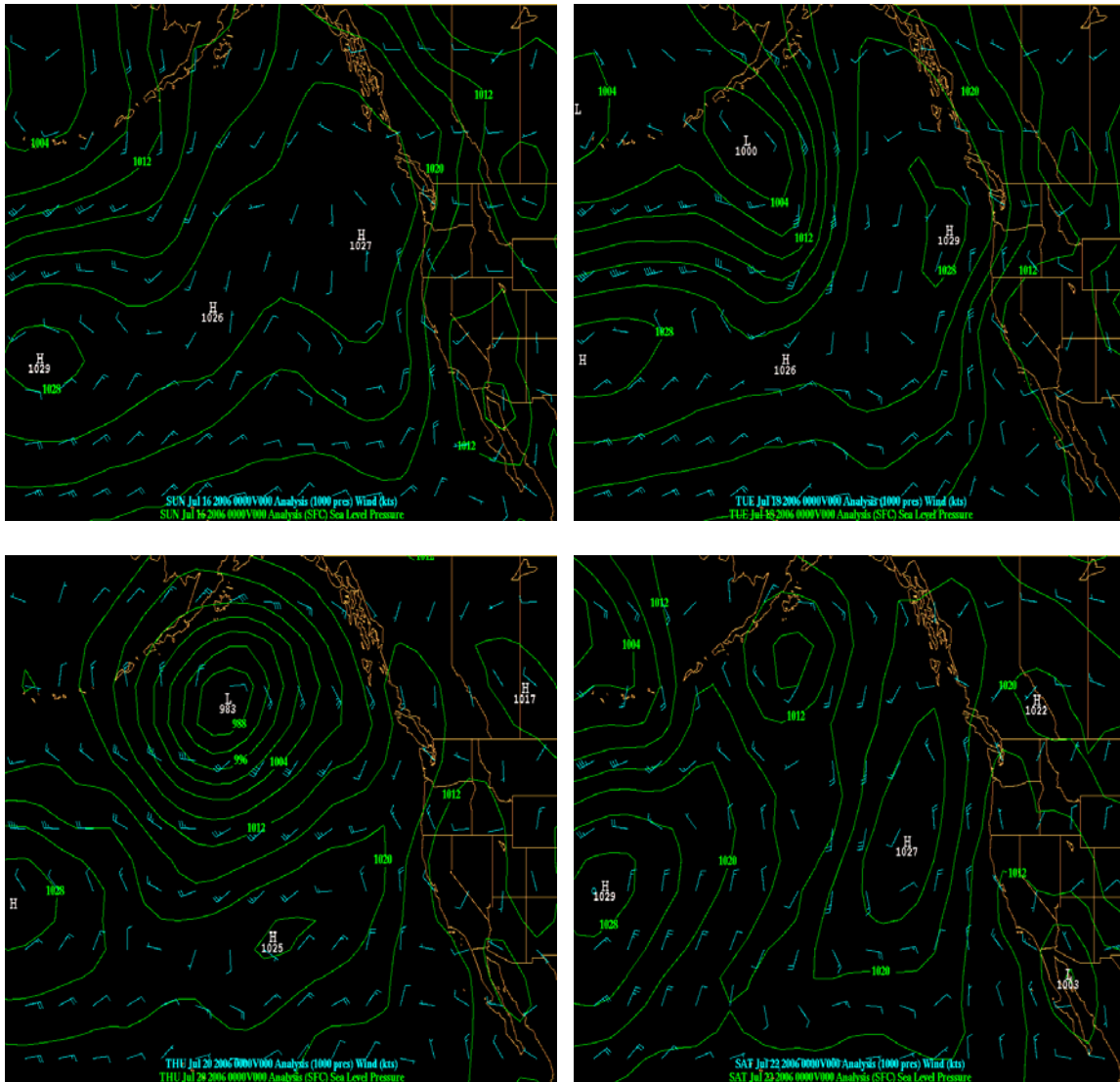


Figure 29 Composites of NCEP GFS model sea level pressure (green) and 1000 mb wind vectors (blue) for July 16, July 18, July 20, and July 22, 2006 analyses. All times are at 0000Z.

2. Coastal Jet Migration

The detachment of the coastal jet from the central California coastline during this case was just as significant as in the previous case. The days leading up to the offshore flow event saw the typical coastal jet features as it hugged the coastline from the Oregon/California state line south to Point Conception then separating from the coast but still continuing its south/southeast trek to below 30 degrees latitude (Fig. 30a). Maximum wind of 15-20 m/s were noted at the typical expansion fan locations downwind from Point Arena and Point Reyes.

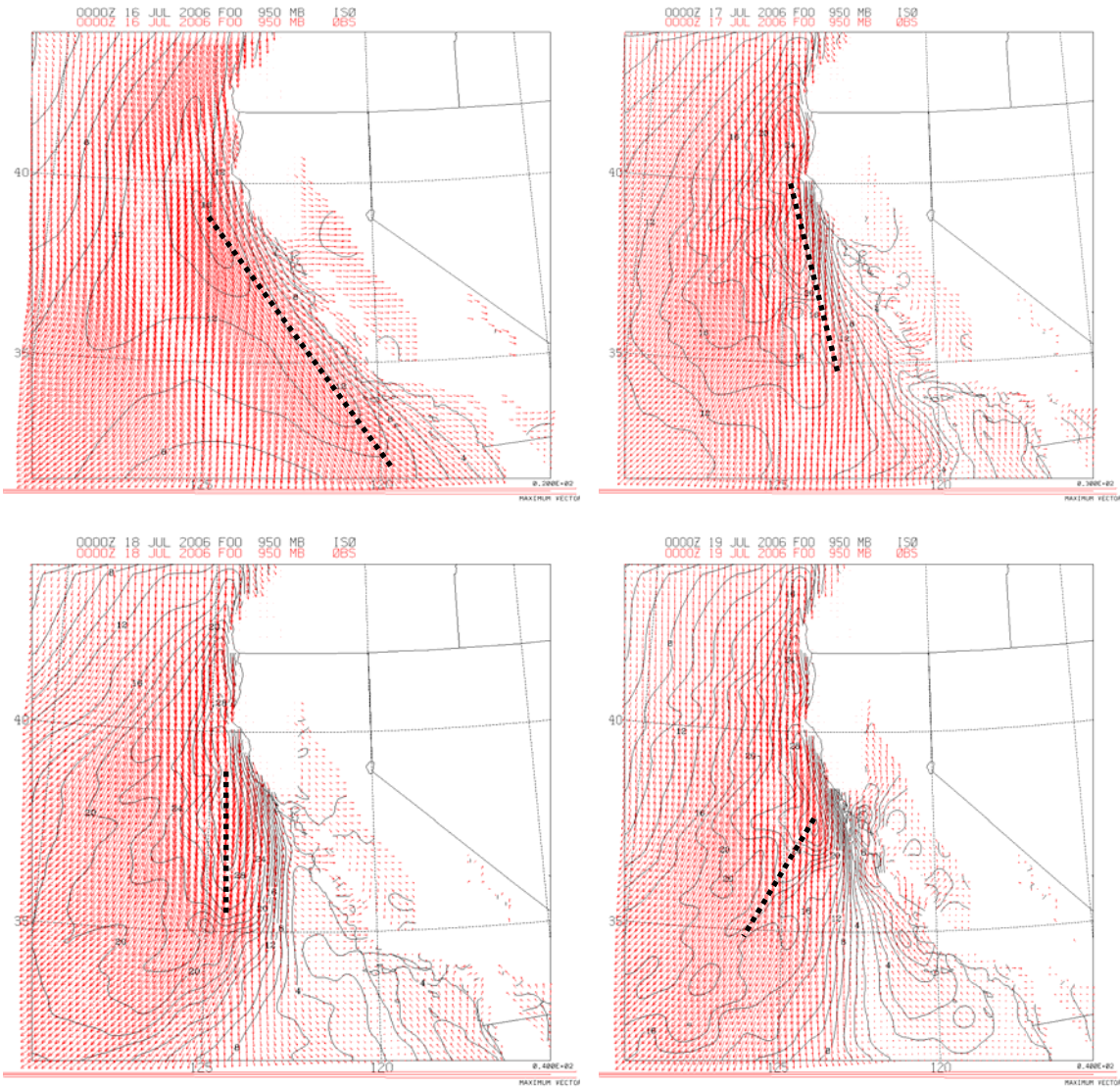


Figure 30. Composite analysis COAMPS™ model 950 mb vector winds (red) and isotachs (solid black) in m/s for July 16-19 at 0000Z. Coastal jet maximum wind axis depicted with dashed black line.

The largest movement westward of the coastal jet occurred during the 48-hour period between July 17 at 0000Z and July 19 at 0000Z. The southern portion of the jet, just offshore from the Santa Lucia, is again where the most movement is seen. From the two cross-sections off the coast of the Santa Lucia (Fig. 31), we find the northwesterly component of the coastal jet winds immediately off the coast to be 8-12 m/s at 000Z on 17 July (Fig. 31a). Forty eight hours later, those winds have died and are showing signs of a southerly surge or coastally trapped wind reversal (Fig. 31b). The northwesterly winds have turned southeasterly at 4-8 m/s, the isentropic gradient is showing signs of loosening and the boundary layer is increasing towards the coast as seen in Figure 31b.

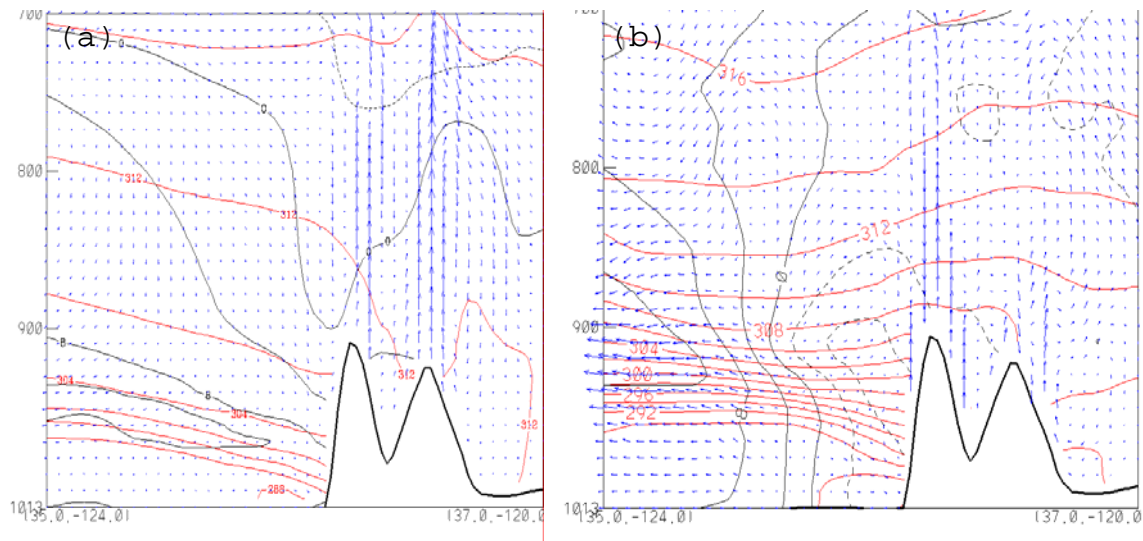


Figure 31. Vertical cross-section COAMPS™ model analysis of cross-section wind vectors (blue), potential temperature in Kelvin (red), and perpendicular to cross-section wind speed (black) in m/s for July 17 and July 19 at 0000Z.

The coastal jet migration is also verified by examining the observed winds at the Cape San Martin buoy 46028. Figure 32 shows a distinct wind shift between July 17 at 1800Z and July 18 at 0000Z. The wind speed at Cape San Martin (Fig. 33) shows light and variable winds continuing for six days until July 22 when the coastal jet migrates back to the coastline resulting in northwest winds of 4-5 m/s at buoy 46028.

Buoy 46028 Cape San Martin Wind Direction (degrees)

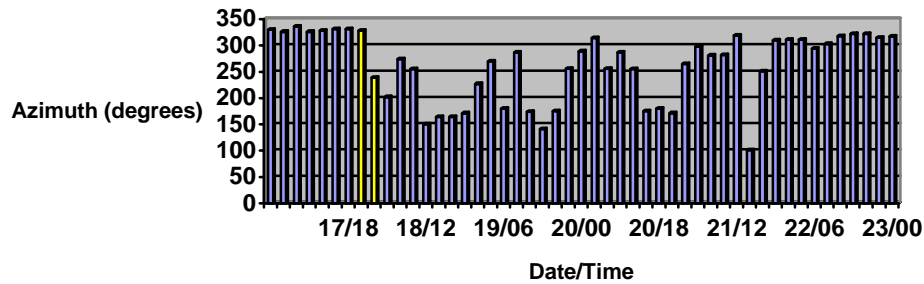


Figure 32. Wind direction in degrees for the period July 17/00Z - July 23/00Z at Buoy 46028 near Cape San Martin. The 6-hour period (July 17, 2100Z - July 18, 0000Z) when windshift occurred is highlighted in yellow.

Buoy 46028 Cape San Martin Wind Speed (kts)

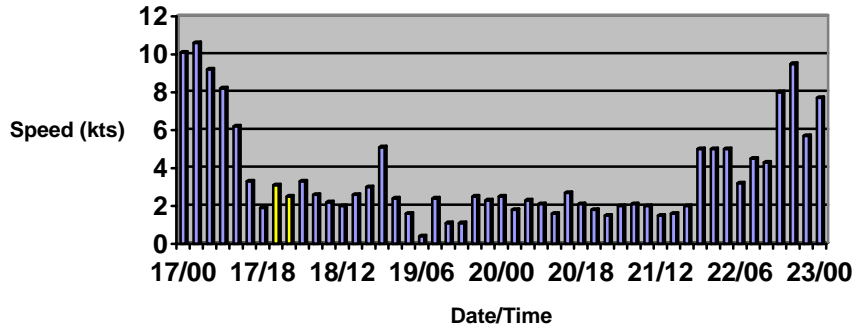


Figure 33. Wind speed in knots for the period July 17/00Z - July 23/00Z at Buoy 46028 near Cape San Martin. The 6-hour period (July 17, 2100Z - July 18, 0000Z) when windshift occurred is highlighted in yellow.

3. Marine Boundary Layer Changes

On July 15, prior to the onset of offshore flow, a cross section of the boundary layer along the Big Sur coastline shows very typical conditions of the boundary layer structure in a typical coastal jet (Fig. 34). Potential temperature surfaces are sloping downward towards the coastline with a jet maximum approximately 70 km off the coastline. The greatest potential temperature gradient is seen close to 960 mb yielding a marine boundary layer depth of approximately 500 m. This is shallower than the initial conditions of the previous case study by approximately 330 m. The maximum winds of 15-20 m/s in the jet core at approximately 950 mb are also weaker than the previous case but still average for the California coastal jet.

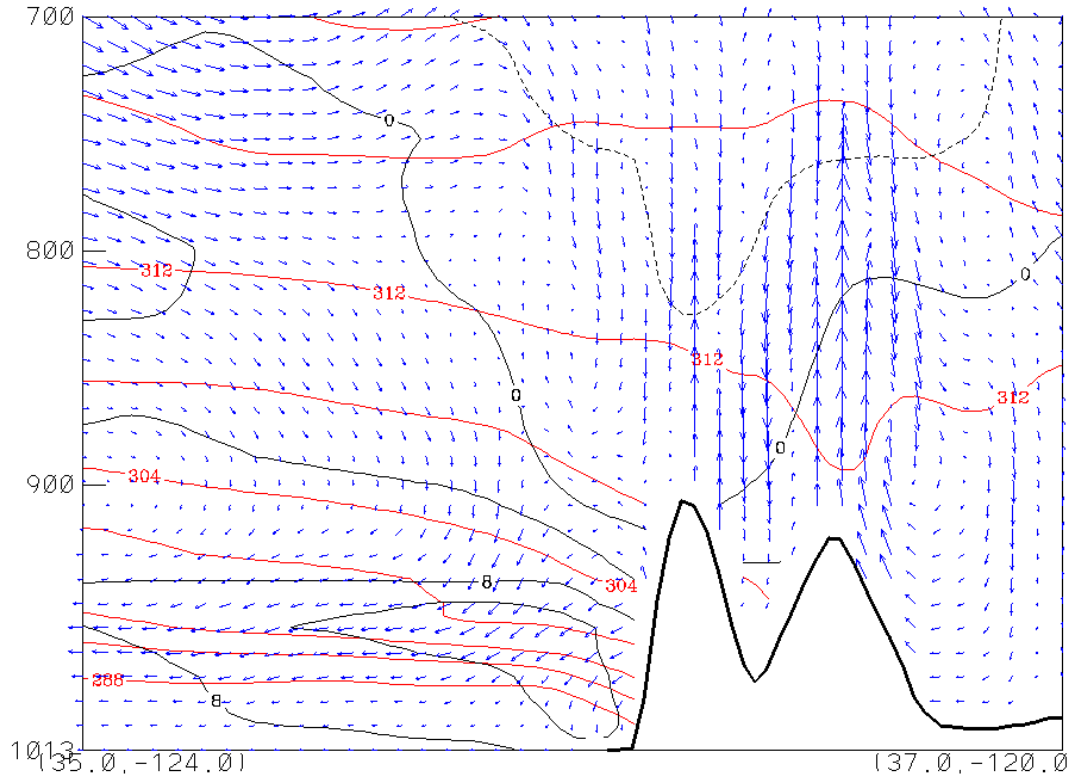


Figure 34. Vertical cross-section COAMPS™ model analysis of cross-section wind vectors (blue), potential temperature in Kelvin (red), and perpendicular to cross-section wind speeds (black) in m/s for July 15 at 0000Z.

By July 18 at 0000Z, the marine boundary layer depth was less than 330 m along the coastline with a more gradual increase in boundary layer depth away from shore (Fig. 35). The main core of offshore winds, unlike the first case study, is occurring well offshore approximately 200-300 km away from the coast. The offshore wind component (AXW) as seen below along the coastal mountains and at ridge top is approaching 0 m/s. This lack of strong cross-coast wind has produced a less favorable region for downsloping wind as the U component is minimal.

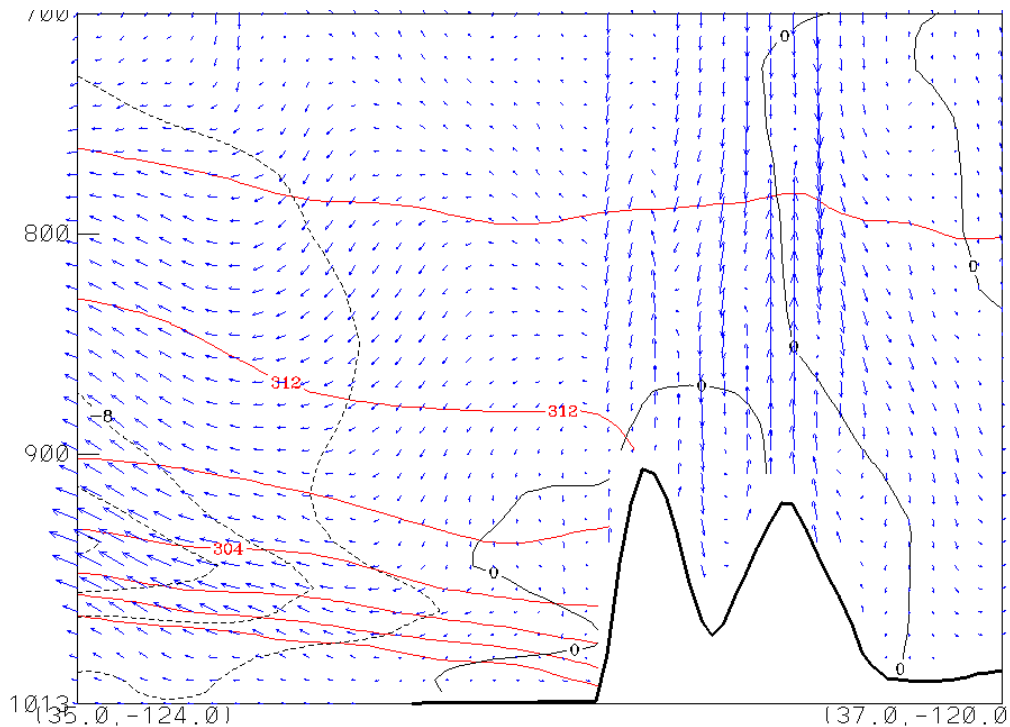


Figure 35. Vertical cross-section COAMPS™ model analysis of cross-section wind vectors (blue), potential temperature in Kelvin (red), and along cross-section wind speed (dashed black) in m/s for June 18 at 0000Z.

This light cross-mountain flow is also evident in the lack of horizontal variability of the compression of the boundary layer downstream from steep terrain. In Figure 36 showing the 950 mb potential temperature analysis and 850 mb wind vectors, the horizontal variability throughout central California is not as significant as in the first case and mountain top winds are nonexistent. This is indicative of the lack of compressional warming of the boundary layer from downsloping winds. Offshore winds at 850 mb across the coastal mountain ranges along the central coast were 2-4 m/s at the strongest point. This light

offshore wind component is leading to a minimal downsloping wind event.

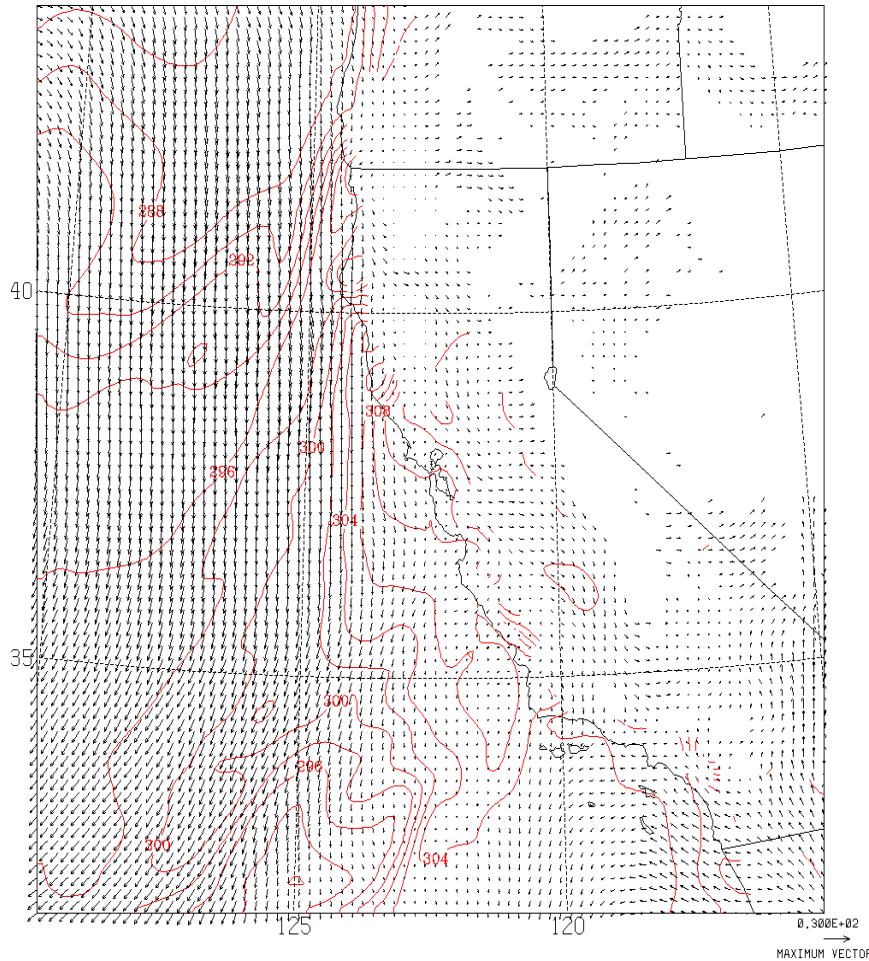


Figure 36. Composite analysis COAMPS™ model 950 mb potential temperatures (red) in Kelvin and 850 mb wind vectors (black) for July 18 at 0000Z.

Because the along coast variability of potential temperature at 950 mb was observed to be more consistent from north to south, the compression of the marine boundary layer is largely due to large-scale subsidence and less caused by compressional warming from cross-coast flow. Figure 37 below compares the 950-700 mb thickness

immediately offshore of the Santa Lucia mountain range along the central coast for both case studies. Comparing the initial stages of both events (Day 1) this July event was almost 60 meters thicker than the June case. Throughout the entire period, in fact, subsidence acting upon the marine boundary layer is stronger and over a broader region than previously seen in June (Figure 37). The greatest increase of 950-700 mb thickness occurred on July 17-18 (Days 2-3) and again correlates strongly to the largest westward migration of the coastal jet (Figure 30).

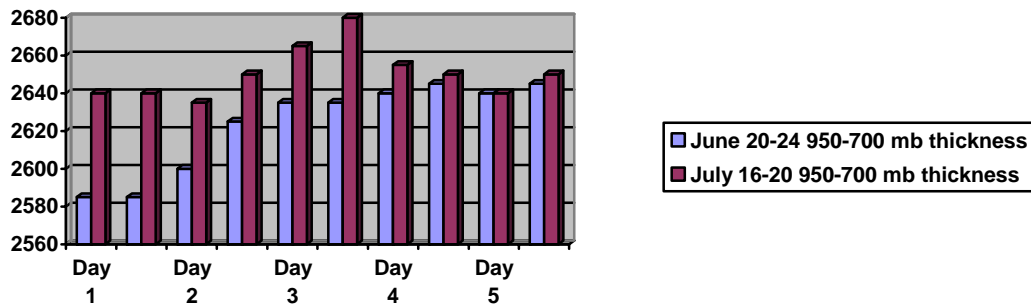


Figure 37. Comparison of 950-700 mb thickness in meters immediately offshore of the Santa Lucia near Pt Sur, California for both case studies.

Figure 38 showing 950-700 mb thickness analysis, a strong west to east thickness gradient is present indicative of the relaxation of subsidence and an increase of marine boundary layer thickness as we progress westward. The tightest thickness gradient is also observed where the strongest winds of the coastal jet occurred. This tight thickness gradient is also consistent with an increase in horizontal potential temperature gradient or steepness in the boundary layer top.

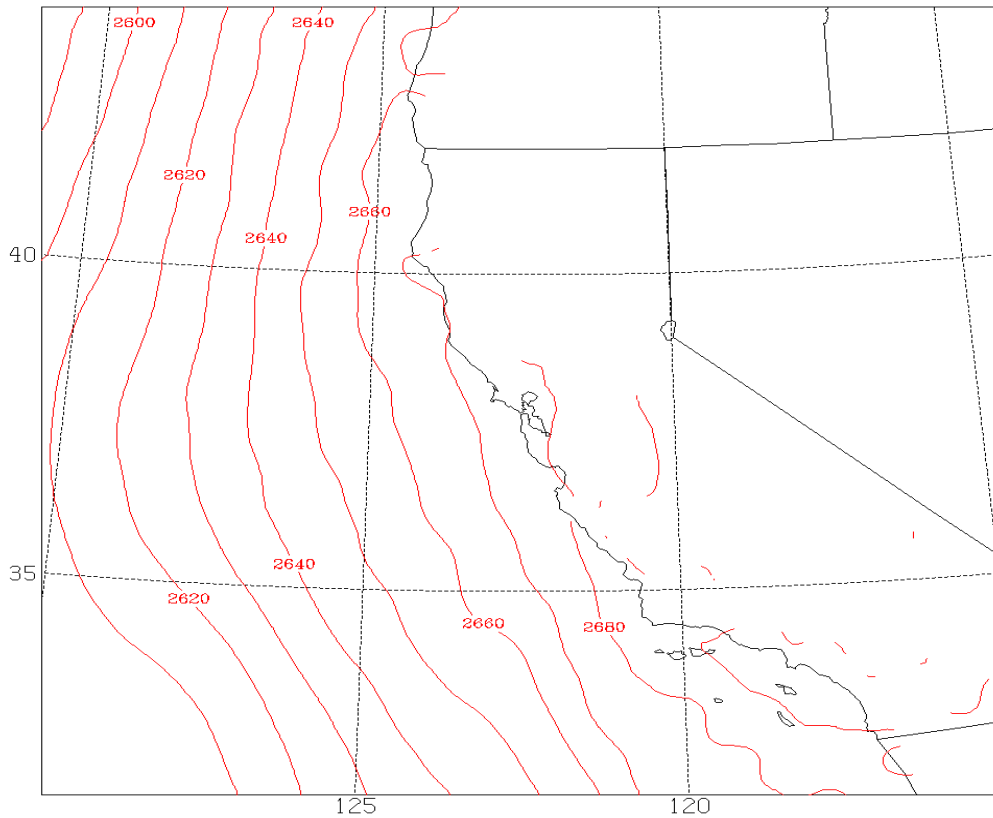


Figure 38. Composite analysis of COAMPS™ model 950 mb through 700 mb thickness for July 18 at 1200Z.

4. July 16-23 Summary

During this case, the major cause of the migration to the west of the coastal jet involved the large area of subsidence. Unlike the first case, the offshore flow was light throughout the period and had a lesser impact on the boundary layer. Offshore winds throughout the first 96-120 hours across the Santa Lucia were only 2-4 m/s as shown by the COAMPS™ analysis. These light offshore winds were again contributed by the migration northeastward of the Pacific High at the surface and the lowering of sea-level pressure off the Southern California Coast from the

westward movement of the thermal trough. The large scale subsidence associated with the strong high pressure throughout the low and mid-levels was the main cause for compression of the boundary layer along the central coast. Both mechanisms, the movement of the horizontal pressure gradient from east to west and, to a much lesser degree, mesoscale boundary layer compression from downsloping winds over the larger coastal mountains again caused the marine boundary layer to decrease in thickness near the coast and become more sloped from east to west at an offshore location. This increase in slope enhanced the horizontal temperature and pressure gradient, leading to separation of the coastal jet from the California coast.

V. CONCLUSIONS/RECOMMENDATIONS

A. CONCLUSIONS

In this study, offshore flow along the central coast of California and its effects on the coastal jet leading to separation from the coastline was investigated during the summer of 2006. Two offshore wind events were narrowed down out of 18 by the duration of cross-coast wind and the degree of coastal jet separation from the coastline. The first case occurred June 20-24, 2006 and began with coastal jet features very typical for a summertime regime off the California coast. Compared with other events throughout the summer it was moderate in length lasting approximately 100 hours. The second case study was a month later occurring July 16-24 with the same mature coastal jet as preconditions immediately along the California coastline. The major findings are summarized below.

First, and in this study the most important aspect leading to separation of the jet from the coastline was low to mid-level subsidence. A direct correlation was found between 950 to 700 mb thickness immediately along the central coast and the initiation of separation of the jet from the coastline. The increase of thickness along the coast acts to compress the marine boundary layer. In both events studied, there was a strong decrease in thickness values to the west which leads to a greater slope in marine boundary layer from east to west. Where the greatest slope of the marine boundary layer was located has, in effect, acted as an eastern border to the coastal jet winds, shifting the core jet westward in both cases. Subsidence

leading to separation of the coastal jet in these two events was easy to forecast. Looking at model output, when low to mid-level thickness values are forecast to increase substantially along and just offshore of the central coast then the forecaster should be alerted to a possible coastal jet separation. In this study, 950-700 mb were the only thickness values used but a variation of this could also be useful. Another aspect of thickness values just as important is the orientation of the gradient. A forecaster needs to look at the orientation of thickness contours. If there is a strong east to west decreasing of thickness values then the boundary layer is more apt to also be sloped upward from east to west, setting up the eastern border of the coastal jet. In both cases, a thickness gradient of 50 m (thickness) : 500 km (y direction) was found to initiate the separation from the coastline. After initiation of separation, the eastern border of the jet was always located where the strongest thickness gradient was located.

The second mechanism leading to the separation of the coastal jet from the California coastline is the intensity of the offshore flow at 850 mb. When the 850 mb up to 500 mb high pressure region, typically placed 300-500 km off the Northern Californian coast, shifts to the northeast towards the Pacific Northwest coastline, offshore winds are possible. This shift of the high pressure region coupled with a westward movement toward the southern California coastline of the thermal trough located in the desert Southwest can reorient the pressure gradient significantly increasing the likelihood of an offshore flow in central California. A forecaster should be alerted to possible

offshore winds along the central coast when this occurs. In the June case there was a significant 850 mb pressure gradient force from northeast to southwest (cross-coast). If a strong enough 850 mb offshore flow is available, and the marine boundary layer inversion is below mountain top level then downsloping wind compression on the boundary layer is likely. In the two cases studied, 850 mb winds of 5 m/s or higher over the Coastal Ranges were found to be enough for significant compression on the marine boundary layer. During the July event, offshore winds at any level were not high enough (5 m/s) for a major impact on the marine boundary layer immediately along the coast. This lack of low to mid-level offshore flow produced minimal compression of the marine boundary layer immediately offshore from the Coastal Ranges. However, there was a significant separation of the coastal jet during the July case study due to low to mid-level subsidence. This leads to the conclusions that the thickness and horizontal temperature and pressure gradient is more likely to lead to separation of the coastal jet than the mesoscale compressional effects of downsloping winds.

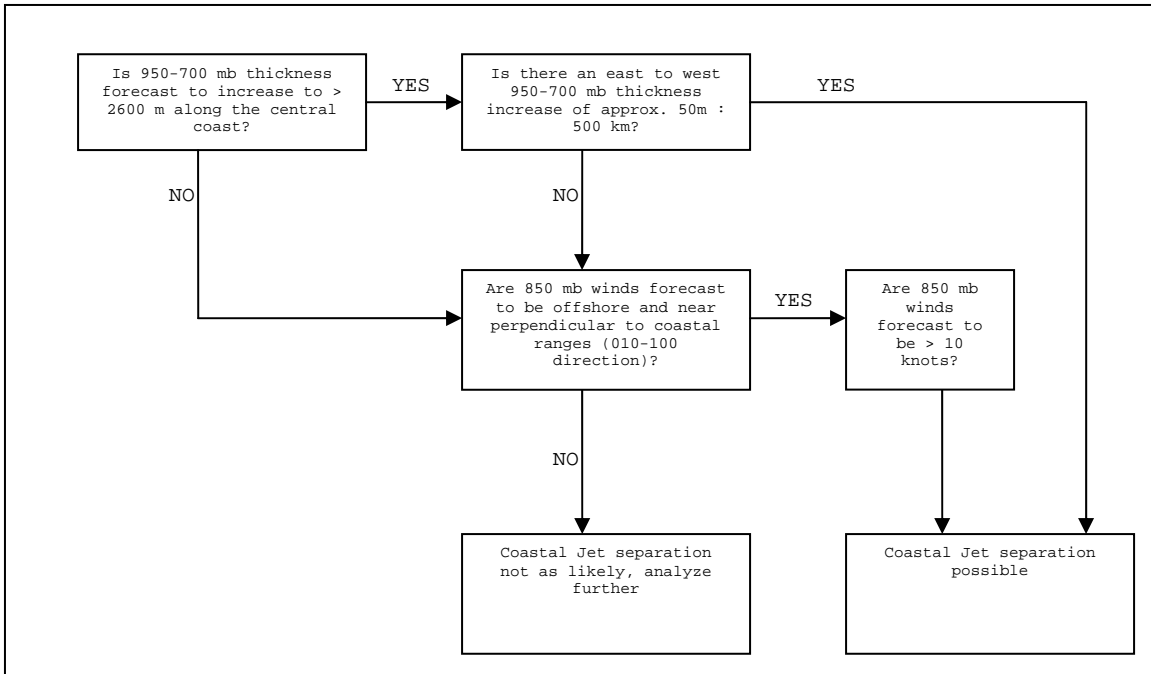


Figure 39. Forecaster decision aid for separation of coastal jet from the Central California coastline.

B. RECOMMENDATIONS

The rules of thumb above were developed with a limited data set for one small region of the Central California Coast during one primary flow direction (offshore). To obtain more accurate guidance an expanded data set of many cases, possibly a decades worth, should be used to fully encompass the entire spectrum of offshore events that have a profound effect on the California Coastal Jet. Many more cases are needed, to continue to verify if these rules of thumb should be maintained, altered, or totally revamped.

Also a concern, that wasn't within the scope of this study, is the effect of the migration westward of the coastal jet on stratus coverage. Stratus coverage, both spatial and temporal, has a large impact on coastal nautical and aviation operations throughout the central

coast and with the groundwork now laid in terms of coastal jet migration, should be included in further research. Possible further study would be to include how the compression of the boundary layer and migration westward of core jet winds affects the coverage of stratus that is usually present in and around the coastal jet.

In this study, the original intent was focusing on offshore wind's effect on the separation of the jet from the coastline. The results were surprising in that an offshore flow was not needed as much as subsidence from the low to mid-level high pressure region in the immediate area. Further case studies and research should be done to see if coastal jet separation is ever observed during other wind flow regimes such as onshore or coast-parallel winds. If subsidence is the main ingredient as concluded in this research than I believe that there are other pressure gradient regimes conducive to coastal jet migration.

THIS PAGE INTENTIONALLY LEFT BLANK

LIST OF REFERENCES

Air Force Combat Climatology Center, cited December 2006:
Strategic Climate Information Service: Operational Climate
Data Summaries for Vandenberg AFB, CA [Available online at
<https://notus2.afccc.af.mil/SCISPublic/>]

Beardsley, R.C., C.E. Dorman, C.A. Friehe, L.K. Rosenfeld,
and C.D. Winant, 1987: Local atmospheric forcing during
the Coastal Ocean Dynamics Experiment: A description of
the marine boundary layer atmospheric conditions over a
Northern California upwelling region. *Journal of
Geophysical Research*, **92**(C2), 1467-1488

Cross, Patrick S., 2003: The California Coastal Jet:
Synoptic Controls and Topographically Induced Mesoscale
Structure. Ph.D. dissertation, Dept of Meteorology, Naval
Postgraduate School, 5-8, 29-30

Hodur, R.M., 1997: The Naval Research Laboratory's Coupled
Ocean/Atmosphere Mesoscale Prediction System (COAMPS).
Monthly Weather Review, **125**, 1414-1430

Jiang, Q., J.D. Doyle and R.B. Smith, 2006: Interaction
between Trapped Waves and Boundary Layers, *Journal of the
Atmospheric Sciences*, 75-102

Maxwell, Brandt, 2007: Analysis of the 22-23 July 2006
Extreme Heat In San Diego County. *Western Regional
Technical Attachment*, No. 07-04, 2-5

NOAA-CIRES Climate Diagnostics Center, cited February 2007:
Monthly/Seasonal climate composites. [Available online at
<http://www.cdc.noaa.gov/>]

Renard, R.J., 2006: Monthly Weather Summaries, Monterey, CA
NWS Forecast Office, [Available online at
http://www.weather.gov/climate/local_data.php?wfo=mtr]

UCAR, cited October 2006: Mountain waves and downsloping
winds. [Available online at
<http://meted.ucar.edu/mesoprim/mtnwave/>]

UCAR, cited November 2006: Operational Models Matrix.
[Available online at
<http://meted.ucar.edu/nwp/pcu2/index.htm>]

UCAR, cited November 2006: Low Level Coastal Jets.
[Available online at
<http://meted.ucar.edu/mesoprim/coastaljet/>]

30th Weather Squadron, Vandenberg AFB, CA, cited December
2006: Forecast Reference Notebook, 4-12

INITIAL DISTRIBUTION LIST

1. Defense Technical Information Center
Ft. Belvoir, Virginia
2. Dudley Knox Library
Naval Postgraduate School
Monterey, California
3. Dr. Wendell A. Nuss
Department of Meteorology
Naval Postgraduate School
Monterey, California
4. Dr. Qing Wang
Department of Meteorology
Naval Postgraduate School
Monterey, California
5. Dr. Phillip Durkee
Department of Meteorology
Naval Postgraduate School
Monterey, California
6. Commander
30th Weather Squadron
Vandenberg AFB, California
7. Director of Operations
30th Weather Squadron
Vandenberg AFB, California
8. Air Force Weather Technical Library
Asheville, North Carolina